A NEW UNIT PROTECTION SCHEME APPLIED TO TRANSMISSION LINES

SUELLEN PAULA DE OLIVEIRA SILVA

PHD THESIS
EM ELECTRICAL ENGINEERING

DEPARTMENT OF ELECTRICAL ENGINEERING

FACULTY OF TECHNOLOGY

UNIVERSITY OF BRASILIA

University of Brasilia
Faculty of Technology
Department of Electrical Engineering

A NEW UNIT PROTECTION SCHEME APPLIED TO TRANSMISSION LINES

Suellen Paula de Oliveira Silva

PHD THESIS SUBMITTED TO THE POSTGRADUATE PROGRAM IN ELECTRICAL ENGINEERING AT THE UNIVERSITY OF BRASILIA AS PART OF THE REQUIREMENTS NECESSARY TO OBTAIN THE DEGREE OF DOCTOR.

APPROVED BY:

Prof. Kleber Melo e Silva, D.Sc. (ENE-UnB)
(Guidance)

Prof. Fernanda Caseño Trindade Arioli. (Unicamp)
(External Examiner)

Prof. Felipe Vigolvino Lopes. (UFPB)
(External Examiner)

Prof. Francis Arody Moreno. (ENE-UnB)
(Internal Examiner)

Brasília/DF, December de 2024.

CATALOG CARD

OLIVEIRA SILVA, SUELLEN PAULA

A NEW UNIT PROTECTION SCHEME APPLIED TO TRANSMISSION LINES. [Brasília/DF] 2024.

PPGEE.TD 210/24., 210 x 297 mm (ENE/FT/UnB, Doctor, PHD THESIS, 2024).

University of Brasilia, Faculty of Technology, Department of Electrical Engineering.

Department of Electrical Engineering

1. Unitary protection
2. Transmission Line
3. Series compensation
4. Fault resistance

I. ENE/FT/UnB
II. Título (série)

BIBLIOGRAPHICAL REFERENCE

OLIVEIRA SILVA, SUELLEN PAULA (2024). A NEW UNIT PROTECTION SCHEME APPLIED TO TRANSMISSION LINES. PHD THESIS, Publicação PPGEE.TD 210/2024, Department of Electrical Engineering, University of Brasilia, Brasilia, DF.

ASSIGNMENT OF RIGHTS

AUTHOR: Suellen Paula Oliveira Silva

TITLE: A NEW UNIT PROTECTION SCHEME APPLIED TO TRANSMISSION LINES.

DEGREE: Doctor YEAR: 2024

Suellen Paula Oliveira Silva

University of Brasilia (UnB)

Darcy Ribeiro Campus

Faculty of Technology - FT

Department of Electrical Engineering(ENE)

Brasília - DF CEP 70919-970

I dedicate this work firstly to God, for being essential in my life, author of my destiny, my guide, present help in times of anguish, to my father Odair José da Silva, my mother Suamaia Silva de Oliveira, to my husband Jackson Vilarinho de Freitas and to my children, who are my base and are always by my side supporting me.

ACKNOWLEDGEMENTS

This study was financed in part by the Coordenação de Aperfeiçoamento de Pessoal de Nível Superior – Brasil (CAPES)

ABSTRACT

Título: A New Unit Protection Scheme Applied to Trasmission Lines.

The present design combines distance and differential protection principles in an innovative way, providing a new transmission line unit protection scheme that is robust to parameters such as fault resistance, loading, source strength, and fault location..The algorithm calculates coefficients Γ_L and Γ_R, and the fault is detected whenever one of these coefficients moves outside a proposed restraint characteristic. It uses a fault phase selection combined with an external fault detection logic that uses a high sampling rate in order to obtain a safe identification of the external fault and a new harmonic restraint strategy, providing reliability for internal faults and safety for external faults, even with CT saturation. To validate its performance, the software Alternative Transients Program was used to simulate the operation of the transmission line when subjected to different operating conditions. The simulations performed were divided into transient analyzes - in which protection behavior is evaluated during short-circuit situations - and parametric sensitivity analyzes, in which the influence of each of the parameters involved in the short circuit is investigated. during the permanent absence regime. The results obtained reveal that the proposed algorithm provides an appropriate, efficient and safe alternative for the protection of transmission lines.

Keywords: Unit protection, fault resistance, transmission line.

RESUMO

Título: Um Novo Esquema de Proteção Unitária Aplicado em Linhas de Transmissão.

O presente projeto combina de princípios de proteção de distância e diferencial de forma inovadora, fornecendo um novo esquema de proteção de unitária de linha de transmissão, de forma que seja robusto a paramêtros como resistência de falta, carregamento, força da fonte e localização do defeito. O algoritmo calcula coeficientes de trip chamados neste trabalho Γ_L e Γ_R, e a falta é detectada sempre que um desses coeficientes se move para fora de uma característica de restrição proposta. Utiliza uma seleção de fase com falta combinada com uma lógica de detecção de falha externa que utiliza uma alta taxa de amostragem a fim de obter uma identificação segura da falta externa e uma nova estratégia de restrição harmônica, fornecendo confiabilidade para falhas internas e segurança para falhas externas, mesmo com saturação de TC. Para validar o seu desempenho, empregou-se o software *Alternative Transients Program* para simular a operação da linha de transmissão quando submetida às diversas condições de operação. As simulações realizadas foram divididas em análises transitórias – nas quais avalia-se o comportamento da proteção durante situações de curto-circuito – e análises de sensibilidade paramétrica, nas quais investiga-se a influência de cada um dos parâmetros envolvidos no curto-circuito durante o regime permanente de falta. Os resultados obtidos revelam que o algoritmo proposto provê uma alternativa apropriada, eficiente e segura para proteção de linhas de transmissão

Palavras-chave: Proteção unitária, resistência de falta, linha de transmissão..

TABLE OF CONTENTS

Table of contents i

List of figures ii

List of tables iii

List of symbols iv

Glossary vii

Chapter 1 – Introduction 1

1.1 Contextualization of the Theme 1
1.2 Motivation 2
1.3 Objectives 2
1.4 Text Organization 3

Chapter 2 – State of the Art Review 4

2.1 State of the Art on Distance Protection with Emphasis on Compensation of the Effect of Fault Resistance 4
2.2 State of the Art on Current Differential Protection 8
2.3 SYNTHESIS OF THE BIBLIOGRAPHICAL REVIEW 13

Chapter 3 – Proposed Algorithm 15

3.1 Coefficients H 15
3.1.1 Calculation of H_L and H_R for Different Types of Fault. 16
3.1.1.1 Three-phase (3P) Faults 16
3.1.1.2 Phase-to- Phase (2P) Faults 17
3.1.1.3 Phase-to-Phase to Ground (2PG) Fault 20
3.1.1.4 Single-Line-to-Ground (SLG) Faults 23
3.1.2 General Expressions for H_L and H_R 26
3.2 Phase Currents Compensation 27

3.3 Faulted Phase Selection . . . 28
3.4 Coefficients $\mathbf{\Gamma}$ . . . 28
3.5 Restraint Characteristic . . . 29
3.6 Overall Description . . . 30
3.6.1 Signal Acquisition . . . 30
3.6.2 Signal Alignment and Scaling . . . 30
3.6.3 Phasor Estimation . . . 30
3.6.4 External Fault Detection . . . 31
3.6.5 Current Compensation . . . 31
3.6.6 Faulted Phase Selection . . . 31
3.6.7 Calculation of H_L and H_R . . . 31
3.6.8 Calculation of Γ_L and Γ_R . . . 31
3.6.9 Trip Decision . . . 32

Chapter 4 – Results 34

4.1 Fault Transient Analysis . . . 34
4.1.1 Case 1 and Case 2 - Fault Transient Analysis - SGL Faults . . . 35
4.1.2 Case 3- Fault Transient Analysis - 2P Fault . . . 42
4.1.3 Case 4- Fault Transient Analysis - 2PG Fault . . . 45
4.1.4 Case 5 - Fault Transient Analysis - 3P Fault . . . 48
4.1.5 Case 6 - Fault Transient Analysis - External Fault . . . 51
4.2 Parametric Sensitivity Analysis . . . 54
4.2.1 PSA.1 - Load variation . . . 57
4.2.2 PSA.2 - Fault Resistance Variation . . . 59
4.2.3 PSA.3 e PSA.4 - Fault Location Variation . . . 62
4.2.4 PSA.5- Source Strength Variation . . . 66

Chapter 5 – Conclusion and Future Investigations 69

References 71

LIST OF FIGURES

3.1 Positive-sequence network for a three-phase fault 16

3.2 Sequence networks for an AB fault. 18

3.3 Sequence networks for an BCG fault. 21

3.4 Sequence networks for an AG fault. 24

3.5 Proposed restraint characteristic. 29

3.6 Block diagram of the proposed algorithm. 33

4.1 Part of the Brazilian power grid, highlighting the 500 kV double circuit series-compensated line between Imperatriz and Presidente Dutra substations. 35

4.2 ATPDraw model of the 500 kV double circuit series-compensated line between Imperatriz and Presidente Dutra substations. 35

4.3 Case 1 - Local currents and voltages for an internal AG fault at 1% of the transmission line. 37

4.4 Case 1 - Remote currents and voltages for an internal AG fault at 1% of the transmission line. 37

4.5 Case 1 - Alpha plane-based phase differential elements. 38

4.6 Case 1 - Proposed algorithm. 38

4.7 Case 1: Algorithms comparison. 39

4.8 Case 2 - Local currents and voltages for an internal AG fault at 129km of the transmission line. 40

4.9 Case 1 - Remote currents and voltages for an internal AG fault at 129km of the transmission line. 40

4.10 Case 2 - Alpha plane-based phase differential elements. 41

4.11 Case 2 - Proposed algorithm. 41

4.12 Case 2: Algorithms comparison. 42

4.13 Case 3 - Local currents and voltages for an internal BC fautl the transmission line. 43

4.14 Case 3 - Remote currents and voltages for an internal BC fault the transmission line. 43

4.15 Case 3 - Alpha plane-based phase differential elements. 44

4.16 Case 3 - Proposed algorithm. 44

4.17 Case 3: Algorithms comparison. 45

4.18 Case 4 - Local currents and voltages for an internal BC fautl the transmission line. 46

4.19 Case 4 - Remote currents and voltages for an internal CAG fault the transmission line. 46

4.20 Case 4 - Alpha plane-based phase differential elements. 47

4.21 Case 4 - Proposed algorithm. 47

4.22 Case 4: Algorithms comparison. 48

4.23 Case 5 - Local currents and voltages for an internal ABC fautl the transmission line. 48

4.24 Case 5 - Remote currents and voltages for an internal ABC fault the transmission line. 49

4.25 Case 5 - Alpha plane-based phase differential elements. 50

4.26 Case 5 - Proposed algorithm. 50

4.27 Case 5: Algorithms comparison. 51

4.28 Case 6 - Local currents and voltages 52

4.29 Case 6 - Remote currents and voltages 52

4.30 Case 6 - Alpha plane-based phase differential elements. 53

4.31 Case 6 - Proposed algorithm. 53

4.32 Case 6 - Algorithms comparison. 54

4.33 Simplified system 55

4.34 PSA.1 - Alpha plane-based phase differential elements. 58

4.35 PSA.1- Proposed algorithm. 58

4.36 PSA.1 - Algorithms comparison. 59

4.37 PSA.2 - Alpha plane-based phase differential elements. 61

4.38 PSA.2- Proposed algorithm. 61

4.39 PSA.2 - Algorithms comparison. 62

4.40 PSA.3 - 3P fault - alpha plane-base phase differential elements. 63

4.41 PSA.3 - 3P fault: proposed algorithm performance. 63

4.42 PSA.3- 3P fault - algorithms comparison. 64

4.43 PSA.4 - AG fault - alpha plane-base phase differential elements. 65

4.44 PSA.4 - AG fault: proposed algorithm performance. 65

4.45 PSA.4 - AG fault: algorithms comparison. 66

4.46 PSA.5- alpha plane-based phase differential elements. 67

4.47 PSA.5 - Proposed algorithm. 67

4.48 PSA.5- algorithms comparison. 68

LIST OF TABLES

2.1 Summary of work related to line distance protection. 9

2.2 Summary of works related to current differential protection for lines. 13

3.1 Loop voltages and currents depending on the faulted phases. 27

4.1 Values assigned to Variables. 56

4.2 Simulated Cases 57

LIST OF SYMBOLS

H_L	coefficient calculated by the proposed algorithm for the local terminal.
H_R	coefficient calculated by the proposed algorithm for the remote terminal.
Γ_L	trip coefficient of the thesis proposal for the local terminal.
Γ_R	trip coefficient of the thesis proposal for the remote terminal..
V_M	Thevenin equivalent voltage source terminal M.
V_N	Thevenin equivalent voltage source terminal N.
$\widehat{I}_L$	Current phasor measured at the local terminal.
$\widehat{I}_R$	Current phasor measured at the remote terminal.
$\widehat{V}_L$	Voltage phasor measured at local terminal.
$\widehat{V}_R$	Voltage phasor measured at remote terminal.
$\widehat{V}_{L1}$	Phasor of the positive sequence voltage seen by the relay at the local terminal.
$\widehat{V}_{L2}$	Phasor of the negative sequence voltage seen by the relay at the local terminal
$\widehat{V}_{L0}$	Phasor of the zero sequence voltage seen by the relay at the local terminal.
$\widehat{I}_{L1}$	Positive sequence current phasor seen by relay at local terminal.
$\widehat{I}_{L2}$	Negative sequence current phasor seen by relay at local terminal.
$\widehat{I}_{L0}$	Zero sequence current phasor seen by relay at local terminal.
$\widehat{V}_{R1}$	Phasor of the positive sequence voltage seen by the relay at the remote terminal.
$\widehat{V}_{R2}$	Phasor of the negative sequence voltage seen by the relay at the remote terminal.

$\widehat{V}_{R0}$	Phasor of the zero sequence voltage seen by the relay at the remote terminal.
$\widehat{I}_{R1}$	Positive sequence current phasor seen by the relay at the remote terminal.
$\widehat{I}_{R2}$	Negative sequence current phasor seen by the relay at the remote terminal.
$\widehat{I}_{R0}$	Zero sequence current phasor seen by the relay at the remote terminal.
$\widehat{I}_{L\phi X}$	Phase compensated currents for local terminal.
$\widehat{I}_{L\phi}$	Phase currents for local terminal.
$\widehat{I}_{L\phi cap}$	Phase charging currents for local terminal.
$\widehat{I}_{L\phi ind}$	Phase shunt reactor currents for local terminal.
C_p	Self capacitance of the transmission line.
C_m	Shunt capacitance of the transmission line.
Z_{ind}	Phase impedance of the shunt reactor.
ϕ	Stand for phases A, B or C.
F_{ext}	External Fault declaration.
K_{harmT}	Sensitivity parameter.
I_{harmT}	Total harmonic restraint current.
$\widehat{V}_{L1}$	Positive sequence voltage phasor at local terminal.
$\widehat{V}_{L2}$	Negative sequence voltage phasor at local terminal.
$\widehat{V}_{L0}$	Zero sequence voltage phasor at local terminal.
$\widehat{I}_{L1}$	Positive sequence current phasor at local terminal.
$\widehat{I}_{L2}$	Negative sequence current phasor at local terminal.
$\widehat{I}_{L0}$	Zero sequence current phasor at local terminal.
h	Percentage of total line length where the fault occurred.
Z_{L1}	Positive sequence impedance per unit length of transmission line.
Z_{L2}	Negative sequence impedance per unit length of transmission line.

Z_{L0}	Zero sequence impedance per unit length of transmission line.
$\widehat{V}_{F1}$	Positive sequence voltage phasor at point F where the fault occurred.
$\widehat{V}_{F2}$	Negative sequence voltage phasor at point F where the fault occurred.
$\widehat{V}_{F0}$	Zero sequence voltage phasor at point F where the fault occurred.
$\widehat{I}_{RN}$	Fasor da corrente de neutro vista pelo relé no terminal remoto.

GLOSSARY

ATP	*Alternative Transients Program*
CTA	Short circuit transient analysis
PAS	Parametric sensitivity analysis
IEEE	*Institute of Electrical and Electronics Engineers*
ONS	National Electric System Operator
SIN	National Interconnected Systeml
SIR	*Source Impedance Ratio*
TL	Transmission Line
CT	Current Transformer
TPC	Capacitive Potential transformer
UnB	University of Brasilia

CHAPTER 1

INTRODUCTION

1.1 CONTEXTUALIZATION OF THE THEME

With the development and growth of society, the demand for energy has been increasing, thus justifying the expansion, modernization and increase in the generation of electrical power systems. In this context, the study of the protection of electrical systems is of utmost importance, in order to guarantee the continuous and safe supply of electrical energy, as well as the interconnection of several subsystems of the national interconnected system (NIS), namely: South, Southeast/Central-West, North and Northeast according to the National Electric System Operator (NOS). This system connects the large generation plants in Brazil in a large transmission network.

Regarding the main electrical components that make up the SIN, transmission lines stand out, which correspond to the most abundant elements, as they are responsible for the interconnection between the generating and consuming units of electrical energy. Due to their physical dimensions, these equipments are exposed to considerable climatic and geographical diversity, which makes them more susceptible to failures.

Lightning strikes, broken conductors, insulation failure, tree branches, fires, voltage surges and vandalism are some of the threats to which a transmission system is subject. In this context, protection systems come into play, constantly monitoring the electrical system to ensure maximum continuity of its operation, so that disturbances are extinguished quickly and appropriately, avoiding the triggering of large-scale power outages (PAINTHANKAR; BHIDE, 2007).

Basically, the transmission line protection system comprises the set of relays, equipment and accessories necessary for the selective detection and elimination of all types of faults and other abnormal operating conditions.

1.2 MOTIVATION

Faults frequently occur during the operation of the electrical power system, which leads to interruptions in the supply of electrical energy to consumers. To this end, a protection system is required to ensure the supply of quality energy. The main function of a protection system is to detect the fault and ensure that the affected parts are disconnected quickly and appropriately, preserving the integrity of the electrical system equipment and preventing further damage from occurring.

Characteristics such as sensitivity, selectivity, speed, reliability and precision need to be dimensioned to meet the needs of the electrical system (ANDERSON, 1999).

Among the different types of protection for transmission lines, distance protection has been the most commonly used, since it requires less complexity of communication channels - since ON/OFF messages are exchanged - which reduces project costs compared to current differential protection that needs to transfer current information (samples or phasors)(ZIEGLER, 2006).However, in recent decades, the increasing use of optical communication systems together with modern numerical relays has culminated in the successful use of current differential protection for transmission lines, even in the case of long lines (ZIEGLER, 2012). The distance function is inherently gradual, however, when associated with a teleprotection scheme, it is capable of providing unitary protection for the line. In addition, other inherently unitary schemes are also widely used, such as the differential function itself.

However, the performance of both distance and differential protection can be negatively affected by different factors, such as fault resistance, load, source intensity. Such factors impair the performance of correct impedance measurement for the distance relay, in differential protection the phase units are close to the sensitivity limit, and may not detect the fault in the transmission line.

1.3 OBJECTIVES

The main objective of this thesis is to propose a new transmission line unitary protection algorithm that is immune to the impact caused by fault resistance and other parameters that

compromise the correct performance of the protection functions. The algorithm calculates a coefficient for local and remote terminals, which are evaluated according to the proposed restraint characteristic in a complex plane. Aiming to improve the safety for external faults, a new harmonic restraint scheme is also proposed. To validate the performance of the proposed scheme, a wide variety of fault scenarios were considered.

The main contributions of this thesis are:

- The proposal combines distance and differential protection principles in an innovative way, providing a new transmission line unit protection scheme.
- It provides reliability for internal faults and safety for external faults, even with CT saturation.
- Robustness in operation regardless of the load, fault type, source strength and fault resistance value.

1.4 TEXT ORGANIZATION

This thesis is organized according to the following structure:

- Chapter 2 presents a survey of the state of the art on differential and distance protection for transmission lines.
- Chapter 3 presents the proposed algorithm, describing its functions and implementations.
- Chapter 4 presents the results and analyses of the simulations performed using the Alternative Transients Program (ATP) software, in which different operating conditions of the electrical system were considered. The analysis of these results is divided into specific cases, which allow the verification of the transient response of the protection evaluated, and analyses of the parametric sensitivity, which allow the investigation of the influence of the parameters related to the short circuit.
- Finally, the final considerations and proposals for the continuation of the thesis project until its conclusion are presented in Chapter 5.

CHAPTER 2

STATE OF THE ART REVIEW

In order to contextualize this thesis proposal regarding the works that discuss distance protection and differential protection of transmission lines, this chapter describes a bibliographic review of the referred topic, together with a concise presentation of the most relevant ideas of some articles related to the subject.

2.1 STATE OF THE ART ON DISTANCE PROTECTION WITH EMPHASIS ON COMPENSATION OF THE EFFECT OF FAULT RESISTANCE

In order to mitigate the error introduced by the fault resistance in the distance function, Eissa (2006) presented a new compensation method based on the calculation of the fault resistance. The calculation of the fault resistance is based on the monitoring of the active power at the relay point. The compensated fault impedance accurately measured the impedance between the relay location and the fault point. The obtained results indicated that the detection of fault resistance can reach 300 Ω and the relay operated correctly for simulated faults within the first, second and third zones and for both symmetric and asymmetric faults.

Filomena *et al.* (2008) proposed a new distance relay algorithm based on phase coordinates and fault resistance estimation. The method was shown to be suitable for balanced and unbalanced systems. The authors concluded that the proposed methodology was not significantly affected by fault resistance or fault location, operating correctly even in extreme situations such as faults with high resistance close to the zone limits and with unbalanced loads

Xu *et al.* (2010) presented a new algorithm for calculating the phase-to-ground and phase-to-phase fault impedance, which can also be extended to three-phase faults. It is different from the traditional distance function method, which assumes that the fault point voltage is zero. The proposed algorithm was derived based on a justifiable assumption that the fault impedance

is purely resistive, which implies that the fault point voltage and the fault current are in phase. The authors highlighted that the proposed algorithm is ideal for distance relaying and was tested using simulations in PSCAD/EMTDC software for a 500 kV transmission line, long or short, with different load levels and fault resistance values. The tests showed that the proposed algorithm was immune to load current and fault resistance.

Makwana & Bhalja (2012) discussed the performance of conventional phase-to-ground distance relay affected due to fault resistance value and power flow direction. The paper presented the problems related to fault resistance. A new distance protection algorithm based on complex impedance plane was proposed, which compensated the errors produced by fault resistance for phase-to-ground short circuits using only local end data. The feasibility of the proposed scheme was tested using MATLAB/SIMULINK software, the simulation results demonstrated the effectiveness of the proposed scheme, since it provides accuracy of the order of 98%.

Song *et al.* (2013) presented an algorithm based on voltage distribution along the transmission line. It was able to mitigate the problems caused by long-distance lines and high fault resistances. The authors developed the distributed parameter line model, which made the proposal suitable for long-distance EHV/UHV transmission lines. High fault resistances were tolerated in the proposed method because the voltage distribution is compensated. In the end, the authors highlighted that this algorithm has low computational complexity. Simulations on distributed parameter transmission line models and field data of the 750 kV line demonstrated the validity and feasibility of the proposed protection method.

Idris *et al.* (2013) showed that fault resistance can cause the Mho distance relay to be underreached. The authors proposed the estimation of the fault location using a two-terminal algorithm. Knowing the fault location, the voltage at the fault point can be calculated using the equivalent sequence network seen from the local terminal. The fault resistance is calculated considering the contribution of the current from the remote terminal. And then the compensation of the fault resistance is made in the apparent impedance calculated by the distance function.

Ma *et al.* (2015) proposed in this paper an adaptive distance protection scheme. First, according to the geometric distribution characteristics of voltage and current in the system, the voltage drop equation from the relay point to the fault location is established, then the

fault location is determined by the phase relationship between the measured current and the measured negative sequence current. The authors then established a new adaptive distance protection criterion formed with the relationship between the fault location and the protection zone. They concluded through simulation tests that the proposed scheme can adaptively modify the distance protection settings, in addition to the proposed algorithm being immune to fault resistance and load current.

Ma *et al.* (2016) described a new line protection scheme for single-phase fault based on phase comparison of voltages. First, according to the phase relationship between the negative sequence current at the relay point and the negative sequence current at the fault point, the angular difference between the measured current and the fault voltage is calculated. Then, with the measured voltage as the reference, the phase angles of the fault point voltage and the compensating voltage are calculated. Then, the line protection criterion was formed according to the phase difference between the fault point voltage and the compensating voltage for in-zone and out-of-zone faults. Simulation tests on the real-time digital simulator were carried out to verify whether the proposed scheme can identify in-zone and out-of-zone faults correctly, unaffected by the fault resistance, source impedance, and system operating condition. In addition, the operating time and setting value error of the proposed protection scheme met the technical requirements of line protection.

Ma *et al.* (2017) proposed a novel adaptive distance protection scheme based on the complex plane impedance. Using the phase relationship between the negative sequence current at the relay point and the current at the fault point, the fault supplementary impedance angle caused by the fault resistance was calculated. Then, the effective fault impedance from the fault point to the relay point was obtained by the trigonometric function ratio of the effective fault impedance, measured impedance, and fault supplementary impedance in the complex plane impedance. On this basis, the adaptive distance protection criterion was constructed. The real-time digital simulator test results demonstrated that the protection scheme proposed in this study is applicable to various types of faults, and has good adaptability to different system operating conditions.

Abdelsalam *et al.* (2018) presented a distance relay that compensates for the effect of high resistance faults during different types of phase-to-ground faults. The authors used a doubly fed

transmission line, which uses the voltages and currents at the local end of the transmission line to measure the proposed impedance. The algorithm was able to accurately measure values for the proposed impedance close to the actual impedance of the faulted part of the transmission line. The simulation results showed the validity of the proposed scheme taking into account the variation of the fault resistance, fault location, and different short-circuit capabilities of the sources.

In Liang *et al.* (2019), fault resistance immunity was improved by utilizing the fault point voltage, measured current, and reaching impedance to construct the virtual measured voltage. Then, a new distance protection scheme, known as protection scheme I, was presented to identify faults inside and outside the protection zone by comparing the amplitudes of the original and virtual measured voltages. Then, the original and virtual measured voltages were improved by a special voltage phasor in phase with the fault point voltage phasor. Based on the improved original and virtual measured voltages, another distance protection scheme is presented, namely, protection scheme II. The two proposed protection schemes are immune to fault resistance and load current and operated well under all types of faults. However, protection scheme II had higher fault detection sensitivity compared to protection scheme I.

Liang *et al.* (2020) presented a new method for calculating line fault impedance. This algorithm differs from the traditional distance protection method, which does not take fault resistance into account. The line fault impedance and fault distance were derived from the geometric relationship between the rotated line fault impedance and the rotated measured impedance, and then the fault distance and line fault impedance were calculated. The method proposed by the authors was immune to fault resistance, insensitive to power angle variations and fault location. It worked well on various types of faults, e.g., AG, BC, BCG, and ABC. The simulation results showed that the proposed method calculated the actual fault distance accurately and identified in-zone and out-of-zone faults correctly.

Zheng *et al.* (2021) show that conventional transmission line distance protection schemes are prone to malfunction under CT saturation. This paper addresses this issue by proposing a novel distance protection scheme that combines the blocking and unblocking criteria of distance protection based on the values ??of differential current, operating voltage, and current harmonic content. The proposed approach is verified by theoretical analysis, dynamic simulation test, and

field operation to ensure that the obtained distance protection is reliable and avoids operating unnecessarily under CT saturation. It is concluded that the proposed approach is capable of reliable operation.

Naidu *et al.* (2023) presented a safe and reliable time-domain distance protection method. The method is applicable to various transmission networks including series-compensated and IBR connected lines. It is computationally simple and fast. The main highlight of the proposed method is that it uses the rate of change of relay current as the operating quantity and compares it with a new dynamically calculated restraint quantity. The testing involved a wide range of fault-related parameters (fault type, loading angle, resistance, location) and SIR. The performance is found to be satisfactory, and the method achieved half-cycle tripping, was unaffected by power swings, CT saturation, and performed well even during simultaneous and evolving faults, and is equally applicable to series-compensated lines.

The papers described in this bibliographic review are classified in Tables 2.1, according to the main aspects analyzed in each of the works cited.

2.2 STATE OF THE ART ON CURRENT DIFFERENTIAL PROTECTION

Tziouvaras *et al.* (2003) and Altuve *et al.* (2004) proposed a differential protection based on the alpha plane, composed of five differential elements: three phase elements and two sequence elements. The operating principles of the alpha plane were discussed and its main advantages and disadvantages in relation to other traditional protections were discussed. In this logic, the phase elements were used in the detection of three-phase faults and in the selection of faulty phases in operations with single-pole reclosing, while the sequence elements were used for asymmetric short circuits, mainly those with high fault resistance. The results obtained indicated that the analyzed alpha plane ensures high sensitivity and safety, in addition to stability for external faults with communication delays or in the presence of saturated CTs.

Benmouyal (2005) investigated the possible trajectories of phase and sequence elements in the alpha plane, under the influence of the following parameters: loading, line length, CT saturation level, fault resistance value, presence of single-pole openings, capacitive current, series compensation and power oscillations. The author stated that phase elements presented finite

Table 2.1. Summary of work related to line distance protection.

Reference	Main aspects analyzed													
	FM	FBT	FB	FT	FIN	FEX	RF	SIR	CARG	LOC	SAT	COMP	ATC	ASP
Eissa (2006)	✓	✓	✓	✓	✓	✓	✓	✓	–	✓	–	–	✓	–
Filomena *et al.* (2008)	✓	✓	–	–	✓	–	✓	–	–	✓	–	–	✓	–
Xu *et al.* (2010)	✓	✓	✓	✓	✓	–	✓	–	✓	✓	–	–	✓	–
Makwana & Bhalja (2012)	✓	✓	✓	✓	✓	–	✓	–	✓	✓	–	–	✓	–
Idris *et al.* (2013)	✓	–	–	–	✓	–	✓	–	–	✓	–	–	✓	–
Song *et al.* (2013)	✓	–	–	–	✓	–	✓	–	–	✓	–	–	✓	–
Ma *et al.* (2015)	✓	–	–	–	✓	–	✓	–	✓	✓	–	–	✓	–
Ma *et al.* (2016)	✓	–	–	–	✓	–	✓	–	✓	✓	–	–	✓	–
Ma *et al.* (2017)	✓	✓	✓	✓	✓	–	✓	–	✓	✓	–	–	✓	–
Abdelsalam *et al.* (2018)	✓	–	–	–	✓	–	✓	✓	✓	✓	–	–	✓	–
Liang *et al.* (2019)	✓	✓	✓	✓	✓	–	✓	–	✓	✓	–	–	✓	–
Liang *et al.* (2020)	✓	✓	✓	✓	✓	✓	✓	–	✓	✓	✓	–	✓	–
Zheng Zheng *et al.* (2021)	✓	✓	–	–	✓	–	–	–	–	✓	✓	–	✓	–
(NAIDU *et al.*, 2023)	✓	✓	✓	✓	✓	✓	✓	✓	✓	✓	✓	✓	✓	✓
Proposed algorithm	✓	✓	✓	✓	✓	✓	✓	✓	✓	✓	✓	✓	✓	✓

Legend:
FM: Single-phase fault ; FB: Two-Phase Fault;
FBT: Two-phase fault-ground; FT: Three-phase fault;
FIN:Internal fault ; FEX: External fault
RF: Fault Resistance; SIR: Font Strength;
ATC:Short Circuit Transient Analysis; LOC: Location of Fault;
CARG: System loading;
ASP: Parametric Sensitivity Analysis

sensitivity to short-circuits with high fault resistance, while sequence elements are independent of this parameter and of the system loading conditions. However, after a single-pole opening, the system becomes unbalanced, which reduces the sensitivity of the sequence elements, thus compromising their performance. To ensure the correct performance of the sequence elements, the author suggested the use of incremental sequence components.

Xu *et al.* (2007) proposed a new algorithm for differential current protection of long extra-high voltage lines, which have high capacitive current. The new relay principle based on the distributed parameter model of the transmission line was used in the scheme, which naturally includes the effect of the distributed capacitive current and does not need to consider its compensation separately. To validate the algorithm, several simulations were performed in systems without compensation and others with series and *shunt* compensation. According to the results obtained, the method operated correctly, since it ensured that the differential protection

analyzed is not affected by the capacitive effect of the line.

Liu *et al.* (2008) This paper proposes an improved current differential protection using numerical solution of partial differential equations (PDEs) that fully considers the distributed parameter characteristics of the transmission line. The numerical experiment validates the effectiveness of the proposed current differential protection. Specifically, the numerical solution method can accurately calculate the current across the entire line. In addition, the proposed current differential protection demonstrates high reliability, safety, sensitivity, operating speed, and low calculation burden.

Miller *et al.* (2010) reviewed existing solutions for the application of differential protection for transmission lines, pointing out the existing restrictions and the necessary adaptations for their best application. The article analyzed differential protection using the alpha plane, addressing aspects of relevance for this type of protection, presenting logic and algorithms for terminals with double circuit breakers, capacitive current compensation, and multi-terminal lines (generalized alpha plane). This production resulted in a tutorial in which the principles of protection, communication and signal processing are discussed together

Xue *et al.* (2013) evaluated the effect of capacitive current on different protections of extra high voltage lines and cables. Thus, some methods of mitigating the capacitive effect were reviewed and discussed, providing general guidelines on the investigated configurations. Among the conclusions, it was highlighted that the differential elements are more influenced by the presence of unbalanced currents and, therefore, presented a more vulnerable operation in an unbalanced system.

Molas *et al.* (2013) described the analytical deductions of the trajectories in the alpha plane for the different types of short circuits. The equations developed showed that in these types of faults the phase elements were influenced by the loading, which does not occur with the sequence elements. The article also highlighted the effect of the capacitive current existing in long lines on the trajectories of the phase and sequence elements and presented results with the removal of the effect of this component.

Silva & Bainy (2016) presented a new generalized alpha plane for numerical differential protection applications. Its performance was evaluated for a wide range of simulated faults in a 500 kV three-terminal transmission line using the Alternative Transients Program (ATP). The

authors pointed out that the obtained results revealed that compared to the only other eneralized alpha plane reported in the literature, the proposed formulation can make the differential protection function have a better behaved response in the alpha plane, in addition to having a simpler formulation.

Almeida & Silva (2017) proposed a new concept for transmission line differential protection based on an incremental complex power alternative alpha plane, in which the restraint characteristic was defined as its left half-plane. The proposed algorithm was inherently phase-segregated, requiring no additional faulted phase selection logic. The proposed harmonic restraint strategy implemented together with the external fault detection logic provides safety for external faults with CT saturation. The performance of the proposed algorithm was tested for a 200 km long 500 kV transmission line using the ATP software. The results obtained revealed that the proposed algorithm provided fast and reliable line protection, being robust against variations in fault parameters, source strengths and loading conditions, as well as power surge situations and line energization maneuvers.

Sarangi & Pradhan (2017) The authors show that the α-plane-based differential relay using phase current has limitations for high resistance faults. It was proposed by the authors to use the phase angle between the voltage and current and the magnitude of the change in current at both ends of a line to confirm an internal fault when the ratio is in the critical region. The adaptive technique was tested for various situations, including series compensated line, high resistance fault, single-pole operation and communication channel delay, and the authors conclude that the performance of the differential protection in the α-plane is improved.

Dantas *et al.* (2018) proposed a time-domain protection solution. In order to provide a deterministic differential protection method, two algorithms were used that use voltage and current samples to estimate the power flow and reactive power entering a protection zone. The algorithms work by integrating time-domain measurements and generated signals in order to achieve stable quantities that are subsequently used for protection. The proposed algorithm was tested in simulations based on data from five real transmission lines; the power systems were simulated using ATP. The authors also described the sensitivity test performed, which included CT saturation and unsynchronized measurements. The proposed solution proved to be safe and reliable under the tested conditions.

Hossain *et al.* (2018) discussed transmission line current differential protection based on the traditional alpha plane that can block the protection actuation while providing greater security for external faults under CT saturation. In this paper, the authors analytically proved that external faults under CT saturation move away from the negative real axis of the complex plane. The proposed alpha plane increases the sensitivity of the line differential protection by unblocking internal faults with the output signal plotted along the negative real axis, without compromising the security for external fault events under CT saturation.

Bainy & Silva (2020) improved the eneralized alpha plane formulation reported in (SILVA; BAINYA, 2016). The main difference is that it is possible to control the region in the alpha plane where the equivalent current ratio stabilizes during the fault period, by correctly configuring only two parameters. To validate and test the performance of the improved eneralized alpha plane, several simulations were performed using ATP in different multiterminal equipment (busbars, transmission lines and power transformers). The results obtained by the authors demonstrated a very stable pre-fault point, and effectiveness of the improved eneralized alpha plane even under severe conditions.

Gupta *et al.* (2020) In this paper, a current differential protection relay for three-phase transmission line is proposed based on the differential approximated coefficients of wavelet transform (DACWT) of three-phase fault currents. The performance of the protection relay is verified for symmetrical faults, asymmetrical faults, external faults, low impedance faults and high impedance faults. It is demonstrated that the protection relay is capable of recognizing the transmission line fault and classifying the faulty phase of the transmission line within 15 ms response time.

Tiferes & Manassero (2022) The proposed algorithm calculates fault probabilities from samples collected by the protection relay. If the developed criteria for pick-up and stability are met, the protection commands actions to open the line. The method can be applied to individual phases of a multiphase transmission line, allowing selective tripping actions. In addition, it implements zero-sequence and negative-sequence time-domain differential protection, using a fractional delay filter to calculate negative-sequence current samples over time. The results obtained indicate that the proposed method is fast and reliable for all types of faults, both under ideal operating conditions and in challenging and critical situations.

The papers described in this bibliographic review are classified in the Tables 2.2 according to the main aspects analyzed in each of the works cited.

Table 2.2. Summary of works related to current differential protection for lines.

Reference	Main aspects analyzed												
	EF	ES	TF	RF	SIR	LOC	CARG	SAT	FIN	FEX	COMP	ATC	ASP
Tziouvaras *et al.* (2003)	✓	✓	✓	✓	–	–	–	✓	✓	✓	✓	✓	–
Altuve *et al.* (2004)	✓	✓	✓	✓	–	–	–	✓	✓	✓	✓	✓	–
Benmouyal (2005)	✓	✓	✓	✓	–	–	✓	✓	✓	✓	–	✓	–
Xu *et al.* (2007)	✓	✓	✓	✓	✓	–	–	–	✓	✓	✓	✓	–
Miller *et al.* (2010)	✓	✓	✓	✓	–	–	✓	✓	✓	✓	–	✓	–
Xue *et al.* (2013)	✓	✓	✓	✓	–	✓	✓	–	✓	–	✓	✓	–
Molas *et al.* (2013)	✓	✓	✓	✓	–	–	✓	–	✓	–	–	✓	–
Silva & Bainy (2016)	✓	–	✓	✓	–	✓	✓	✓	✓	✓	–	✓	✓
Almeida & Silva (2017)	✓	–	✓	✓	✓	✓	✓	✓	✓	✓	–	✓	✓
Sarangi & Pradhan (2017)	✓	✓	✓	✓	✓	✓	✓	✓	✓	✓	✓	✓	–
Dantas *et al.* (2018)	✓	✓	✓	✓	–	–	✓	✓	✓	✓	–	✓	–
Hossain *et al.* (2018)	✓	–	✓	–	–	–	–	✓	✓	✓	–	✓	–
Bainy & Silva (2020)	✓	–	✓	✓	✓	✓	✓	✓	✓	✓	–	✓	✓
Gupta *et al.* (2020)	✓	–	✓	✓	–	✓	–	–	✓	✓	–	✓	–
Tiferes & Manassero (2022)	✓	–	✓	✓	–	✓	–	✓	✓	✓	–	✓	–
Liu *et al.* (2008)	✓	–	✓	✓	–	–	–	–	✓	✓	–	✓	–
Proposed algorithm	✓	✓	✓	✓	✓	✓	✓	✓	✓	✓	✓	✓	✓

Legend:
ATC: Short Circuit Transient Analysis;
ASP: Parametric sensitivity analysis;
EF:Phase elements;
COMP:Series compensation;
ES:Sequence elements;
CARG: System loading; RF: Fault resistance;
SIR: Source strength; LOC: Location of the fault;
FIN: Internal fault FEX: External fault
ES: Sequence elements; TF: Type of fault;
SAT: CT saturation

2.3 SYNTHESIS OF THE BIBLIOGRAPHICAL REVIEW

Regarding the studies related to distance protection in transmission lines, all of them addressed an important aspect that affects the good performance of the distance function, which is the fault resistance. This parameter compromises the integrity of transmission lines

for short circuits that are not direct. The studies indicated the possible solutions that ensure the adequate performance of the distance protection. Regarding the disadvantages of distance protection, the sensitivity of this method to the line parameters stands out; the distance function is sensitive to the system loading, source strength and fault resistance. In addition, the method is not capable of providing unitary protection to the protected element, and due to errors caused by any of the parameters reported above, the relay may overreach or underreach, and may act for a short circuit external to the transmission line.

In the works related to current differential protection in transmission lines, important aspects related to this type of protection were addressed, with regard to the characteristics of communication between differential relays, the criteria for implementing the alpha plane and the advantages of using this strategy. These works also highlighted situations in which the protection may act incorrectly, indicating possible solutions that ensure the adequate operation of the current differential protection. Some disadvantages associated with the use of current differential protection can be noted, such as the difficulty in determining the restriction characteristic in the alpha plane, which depends on adjustments related to the presence of, for example, a saturated CT.

Considering the above-mentioned aspects, this thesis proposes a new algorithm for unitary protection of transmission lines, which combines distance and differential protection principles in an innovative way,for this purpose it makes an estimate of the fault location for each fault loop, this is a characteristic of the distance function that through the measured impedance the location of the defect is obtained, in the calculation of this location estimate named in this work as H_L and H_L the sum of the current of both terminals of the line appears, a characteristic also present in differential protection, as well as the use of the operating current to correctly select the faulted phase. The algorithm calculates a coefficient for local and remote terminals, which are evaluated according to the proposed restraint characteristic in a complex plane. Aiming to improve the safety for external faults, a new harmonic restraint scheme is also proposed. To validate the performance of the proposed scheme, a wide variety of fault scenarios were considered. The obtained results reveal that the proposed algorithm is quite robust to fault resistance and provides a reliable and safe alternative for transmission line protection.

CHAPTER 3

PROPOSED ALGORITHM

This chapter presents the proposed algorithm, which aims to promote the unitary protection of the transmission line, innovatively combining the characteristics of distance protection, which is the fact of estimating the location of the fault according to the fault loop, as well as the characteristics of differential protection, in this case the reading of the current at the two terminals of the transmission line, as well as the faulted phase selection criterion based on the TL operating current..

The proposed algorithm, that uses voltages and currents at line terminals to calculate coefficients H, which represent fault location estimations in per unit of the line length. Then, new coefficients Γ are computed using coefficients H, and employing an harmonic restraint strategy to provide security for CT saturation during external faults. A trip command is issued whenever either local or remote coefficients Γ moves outside the proposed restraint characteristic, which is defined as an unit radius circle centered at the origin.

3.1 COEFFICIENTS H

For the sake of simplicity, only the mathematical formulation for local terminal coefficient H_L is presented. It should be noted that calculations for H_R are analogous. The subscripts L and R stand for local and remote line terminals, respectively, whereas subscripts 0, 1 and 2 stand for zero-, positive- and negative-sequence symmetrical components, respectively. The following sections describe the coefficient H_L for different fault typs.

3.1.1 Calculation of H_L and H_R for Different Types of Fault.

3.1.1.1 Three-phase (3P) Faults

In the case of a 3P fault that takes place at percentage h of the line from its local terminal, only positive sequence network is taken into account, as shown in Figure 3.1.

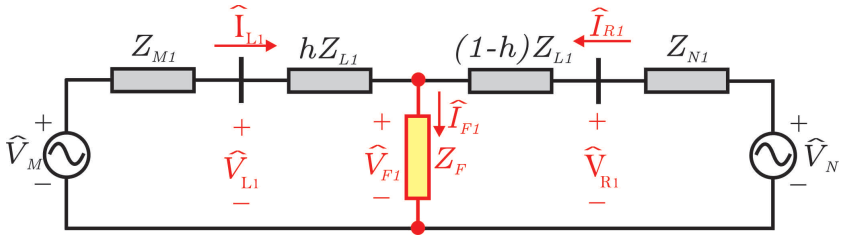

Figure 3.1. Positive-sequence network for a three-phase fault

.

The positive sequence voltage seen by the relay at both terminals of the transmission line is then obtained, defined as:

$$\widehat{V}_{L1} = hZ_{L1}\hat{I}_{L1} + \widehat{V}_{F1} \tag{3.1}$$

$$\widehat{V}_{R1} = (1-h)Z_{L1}\hat{I}_{R1} + \widehat{V}_{F1} \tag{3.2}$$

For this type of short circuit, the unit responsible for identifying the short circuit will be the AB phase unit, so that the voltage at the local and remote terminals are as follows:

- Voltage drop $\widehat{V}_{LAB}$ at local terminal:

$$\widehat{V}_{LAB} = \widehat{V}_{LA} - \widehat{V}_{LB} = hZ_{L1}\hat{I}_{L1} + \widehat{V}_{F1} - a^2hZ_{L1}\hat{I}_{L1} + a^2\widehat{V}_{F1} \tag{3.3}$$

It is known that:

$$\widehat{I}_{LA} = \widehat{I}_{L1} \tag{3.4}$$

$$\widehat{I}_{LB} = a^2\widehat{I}_{L1} \tag{3.5}$$

then we obtain the current $\widehat{I}_{LAB}$:

$$\widehat{I}_{LAB} = (1-a^2)\widehat{I}_{L1} \tag{3.6}$$

Substituting Equation (3.6) into (3.3), we arrive at the voltage drop $\widehat{V}_{LAB}$:

$$\widehat{V}_{LAB} = hZ_{L1}\hat{I}_{LAB} + (1-a^2)\widehat{V}_{F1} \tag{3.7}$$

In a similar manner, the voltage drop $\widehat{V}_{AB}$ seen at the remote terminal is obtained.

- Voltage drop $\widehat{V}_{RAB}$ at remote terminal:

$$\widehat{V}_{RAB} = \widehat{V}_{RA} - \widehat{V}_{RB} = (1-h)Z_{L1}\hat{I}_{R1} + \widehat{V}_{F1} - a^2(1-h)Z_{L1}\hat{I}_{R1} + a^2\widehat{V}_{F1} \tag{3.8}$$

It is known that:

$$\widehat{I}_{RA} = \widehat{I}_{R1} \tag{3.9}$$

$$\widehat{I}_{RB} = a^2\widehat{I}_{R1} \tag{3.10}$$

then we obtain the current $\widehat{I}_{RAB}$:

$$\widehat{I}_{RAB} = (1-a^2)\widehat{I}_{R1} \tag{3.11}$$

Substituting Equation ((3.11) into (3.8), we arrive at the voltage drop $\widehat{V}_{RAB}$:

$$\widehat{V}_{RAB} = (1-h)Z_{L1}\hat{I}_{RAB} + (1-a^2)\widehat{V}_{F1} \tag{3.12}$$

With the voltage drop equations $\widehat{V}_{AB}$ at both LT terminals, the local voltage drop is then subtracted from the remote voltage drop, obtaining the following equation:

$$\widehat{V}_{LAB} - \widehat{V}_{RAB} = hZ_{L1}(\widehat{I}_{LAB} + \widehat{I}_{RAB}) - Z_{L1}\hat{I}_{RAB} \tag{3.13}$$

Naming the parcel $\widehat{I}_{LAB} + \widehat{I}_{RAB}$ of $\widehat{I}_{Dif,AB,3\phi}$ and isolating the variable h, we obtain:

$$H_{LAB} = \frac{(\widehat{V}_{LAB} - \widehat{V}_{RAB}) + Z_{L1}\hat{I}_{RAB}}{Z_{L1}\hat{I}_{Dif,AB,3\phi}} \tag{3.14}$$

3.1.1.2 Phase-to- Phase (2P) Faults

In the case of a two-phase fault (BC), the interconnection of the sequence circuits is illustrated in Figure 3.2. Subscripts 1 and 2 indicate, respectively, the positive and negative sequence components. This type of fault, considered unbalanced, affects two phases of the system; only the positive and negative sequence components of the voltage and current phasors are analyzed.

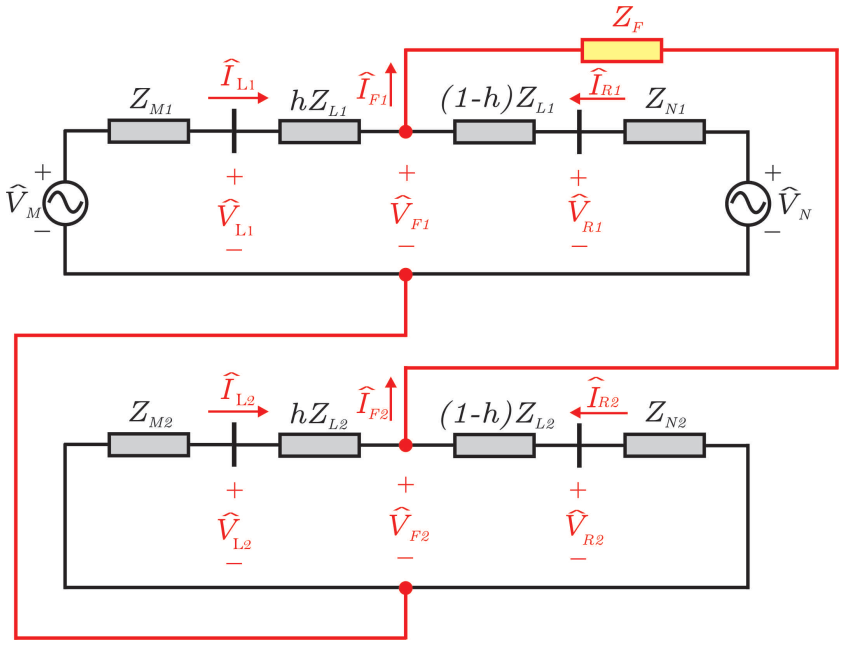

Figure 3.2. Sequence networks for an AB fault.

.

As done for the three-phase short-circuit, the voltage drop at both ends of the transmission line is equated $\widehat{V}_{BC}$.

- Voltage drop $\widehat{V}_{LBC}$ at Local terminal:

The voltage drop at the local terminal is calculated as follows $\widehat{V}_{LBC} = \widehat{V}_{LB} - \hat{V}_{LC}$.

$$\widehat{V}_{LB} = a^2\widehat{V}_{L1} + a\widehat{V}_{L2} \tag{3.15}$$

$$\widehat{V}_{LC} = a\widehat{V}_{L1} + a^2\widehat{V}_{L2} \tag{3.16}$$

Knowing that:

$$\widehat{V}_M = (Z_{M1} + hZ_{L1})\widehat{I}_{L1} + \widehat{V}_{F1} - (Z_{M2} + hZ_{L2})\widehat{I}_{L2} \tag{3.17}$$

$$\widehat{V}_{L1} = \widehat{V}_M - Z_{M1}\widehat{I}_{L1} = hZ_{L1}\widehat{I}_{L1} + \widehat{V}_{F1} - (Z_{M2} + hZ_{L2})\widehat{I}_{L2} \tag{3.18}$$

$$\widehat{V}_{L2} = -Z_{M2}\widehat{I}_{L2} \tag{3.19}$$

Substituting Equations (3.18) and (3.19) into equation (3.15), we obtain the local voltage in phase B and C:

$$\widehat{V}_{LB} = a^2hZ_{L1}\widehat{I}_{L1} + a^2\widehat{V}_{F1} - a^2hZ_{L1}\widehat{I}_{L2} - a^2Z_{M2}\widehat{I}_{L2} - aZ_{M2}\widehat{I}_{L2} \tag{3.20}$$

$$\widehat{V}_{LC} = ahZ_{L1}\widehat{I}_{L1} + a\widehat{V}_{F1} - ahZ_{L1}\widehat{I}_{L2} - aZ_{M2}\widehat{I}_{L2} - a^2Z_{M2}\widehat{I}_{L2} \tag{3.21}$$

With the voltages of phases B and C, the voltage drop for the local terminal $\widehat{V}_{LBC}$ is then calculated.

$$\widehat{V}_{LBC} = \widehat{V}_{LB} - \widehat{V}_{LC} = (a^2 - a)hZ_{L1}\widehat{I}_{L1} + (a - a^2)hZ_{L1}\widehat{I}_{L2} + (a^2 - a)\widehat{V}_{F1}. \tag{3.22}$$

It is known that:

$$\hat{I}_{LB} = a^2\hat{I}_{L1} + a\hat{I}_{L2} \tag{3.23}$$

$$\hat{I}_{LC} = a\hat{I}_{L1} + a^2\hat{I}_{L2} \tag{3.24}$$

then it is known that $\hat{I}_{LBC}$:

$$\hat{I}_{LBC} = (a^2 - a)\hat{I}_{L1} + (a - a^2)\hat{I}_{L2} \tag{3.25}$$

Substituting Equation (3.25) into Equation (3.22):

$$\widehat{V}_{LBC} = \widehat{V}_{LB} - \hat{V}_{LC} = hZ_{L1}\widehat{I}_{LBC} + (a^2 - a)\widehat{V}_{F1} \tag{3.26}$$

Likewesi to the equation for the voltage $\widehat{V}_{BC}$ for the local terminal, we find the equation for the voltage drop BC for the remote terminal:

- Voltage drop $\widehat{V}_{RBC}$ at remote terminal:

The BC voltage drop seen by the remote terminal is calculated $\widehat{V}_{RBC} = \widehat{V}_{RB} - \hat{V}_{RC}$.

$$\widehat{V}_{RB} = a^2\widehat{V}_{R1} + a\widehat{V}_{R2} \tag{3.27}$$

$$\widehat{V}_{RC} = a\widehat{V}_{R1} + a^2\widehat{V}_{R2} \tag{3.28}$$

According to the Figure 3.2 we have that:

$$\widehat{V}_N = (Z_{N1} + (1 - h)Z_{L1})\widehat{I}_{R1} + \widehat{V}_{F1} - (Z_{N2} + (1 - h)Z_{L2})\widehat{I}_{R2} \tag{3.29}$$

$$\widehat{V}_{R1} = \widehat{V}_N - Z_{N1}\widehat{I}_{R1} = (1 - h)Z_{L1}\widehat{I}_{R1} + \widehat{V}_F - (1 - h)Z_{L2}\widehat{I}_{R2} - Z_{N2}\widehat{I}_{R2} \tag{3.30}$$

$$\widehat{V}_{R2} = -Z_{M2}\widehat{I}_{R2} \tag{3.31}$$

Substituting Equations (3.30) and (3.31) into Equations (3.27) and (3.28), we obtain the remote voltage in phase B and C:

$$\widehat{V}_{RB} = a^2(1 - h)Z_{L1}\widehat{I}_{R1} + a^2\widehat{V}_{F1} - a^2(1 - h)Z_{L1}\widehat{I}_{R2} - a^2Z_{M2}\widehat{I}_{R2} - aZ_{M2}\widehat{I}_{L2} \tag{3.32}$$

$$\widehat{V}_{LC} = a(1-h)Z_{L1}\widehat{I}_{R1} + a\widehat{V}_{F1} - a(1-h)Z_{L1}\widehat{I}_{R2} - aZ_{M2}\widehat{I}_{R2} - a^2 Z_{M2}\widehat{I}_{L2} \tag{3.33}$$

Using the voltages of phases B and C, the voltage drop for the local terminal $\widehat{V}_{LBC}$ is then calculated.

$$\widehat{V}_{RBC} = \widehat{V}_{RB} - \widehat{V}_{RC} = (a^2-a)(1-h)Z_{L1}\widehat{I}_{R1} + (a-a^2)(1-h)Z_{L1}\widehat{I}_{R2} + (a^2-a)\widehat{V}_{F1}. \tag{3.34}$$

It is known that:

$$\hat{I}_{RB} = a^2\hat{I}_{R1} + a\hat{I}_{R2} \tag{3.35}$$

$$\hat{I}_{RC} = a\hat{I}_{R1} + a^2\hat{I}_{R2} \tag{3.36}$$

then it is known that $\hat{I}_{RBC}$:

$$\hat{I}_{RBC} = (a^2-a)\hat{I}_{R1} + (a-a^2)\hat{I}_{R2} \tag{3.37}$$

Substituting Equation (3.37) into (3.34), we then obtain $\widehat{V}_{RBC}$:

$$\widehat{V}_{RBC} = \widehat{V}_{RB} - \widehat{V}_{RC} = hZ_{L1}\widehat{I}_{RBC} + (a^2-a)\widehat{V}_{F1} \tag{3.38}$$

Having obtained the voltage drop equations $\widehat{V}_{BC}$ at both LT terminals, the local voltage drop is then subtracted from the remote one, obtaining the following equation:

$$\widehat{V}_{LBC} - \widehat{V}_{RBC} = hZ_{L1}(\widehat{I}_{LBC} + \widehat{I}_{RBC}) - Z_{L1}\hat{I}_{RBC} \tag{3.39}$$

Naming the portion $\widehat{I}_{LBC} + \widehat{I}_{RBC}$ of $\widehat{I}_{Dif,BC,2\phi}$ and isolating the variable h, we then find the coefficient H:

$$H_{LBC} = \frac{(\widehat{V}_{LBC} - \widehat{V}_{RBC}) + Z_{L1}\hat{I}_{RBC}}{Z_{L1}\hat{I}_{Dif,BC,2\phi}} \tag{3.40}$$

3.1.1.3 Phase-to-Phase to Ground (2PG) Fault

The two-phase earth fault shown in Figure 3.3 has three positive, negative and zero sequence networks.

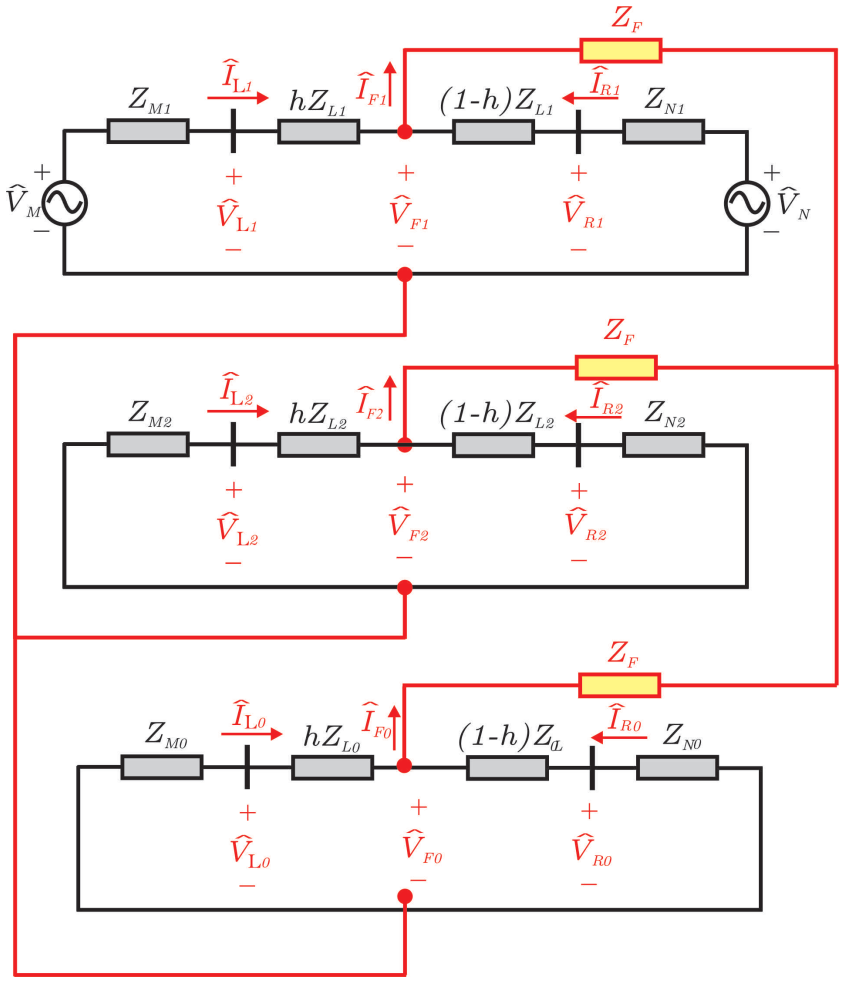

Figure 3.3. Sequence networks for an BCG fault.

.

From the circuit in Figure 3.3, the voltage drop $\widehat{V}_{BCT}$ across both terminals of the LT is then equated.

- Voltage drop $\widehat{V}_{BCT}$ at Local terminal:

From the circuit illustrated in Figure 3.3 we obtain the following equation:

$$\widehat{V}_M = (Z_{M1} + hZ_{L1})\widehat{I}_{L1} + \widehat{V}_{F1} - \widehat{V}_{F2} - (Z_{M2} + hZ_{L2})\widehat{I}_{L2} \tag{3.41}$$

Knowing that:

$$\widehat{V}_{L0} = -Z_{M0}\widehat{I}_{L0} \tag{3.42}$$

$$\widehat{V}_{L1} = \widehat{V}_M - Z_{M1}\widehat{I}_{L1} = hZ_{L1}\widehat{I}_{L1} + \widehat{V}_{F1} - \widehat{V}_{F2} - (Z_{M2} + hZ_{L2})\widehat{I}_{L2} \tag{3.43}$$

$$\widehat{V}_{L2} = -Z_{M2}\widehat{I}_{L2} \tag{3.44}$$

One can calculate the voltage drop $\widehat{V}_{LBCT}$ given by $\widehat{V}_{LBCT} = \widehat{V}_{LB} - \widehat{V}_{LC}$, where:

$$\widehat{V}_{LB} = \widehat{V}_{L0} + a^2\widehat{V}_{L1} + a\widehat{V}_{L2} \tag{3.45}$$

$$\widehat{V}_{LC} = \widehat{V}_{L0} + a\widehat{V}_{L1} + a^2\widehat{V}_{L2} \tag{3.46}$$

We substitute in Equatioon (3.45) and (3.46) the Equations (3.42), (3.43) and (3.44), and we obtain the following expressions:

$$\widehat{V}_{LB} = -Z_{M0}\widehat{I}_{L0} + a^2hZ_{L1}\widehat{I}_{L1} + a^2\widehat{V}_{F1} - a^2\widehat{V}_{F2} - a^2hZ_{L1}\widehat{I}_{L2} - a^2Z_{M2}\widehat{I}_{L2} - aZ_{M2}\widehat{I}_{L2}. \tag{3.47}$$

$$\widehat{V}_{LC} = -Z_{M0}\widehat{I}_{L0} + ahZ_{L1}\widehat{I}_{L1} + a\widehat{V}_{F1} - a\widehat{V}_{F2} - ahZ_{L1}\widehat{I}_{L2} - aZ_{M2}\widehat{I}_{L2} - a^2Z_{M2}\widehat{I}_{L2}. \tag{3.48}$$

Using the voltages in phases B and C, calculate the voltage drop seen at the local terminal $\widehat{V}_{LBCT}$:

$$\widehat{V}_{LBCT} = \widehat{V}_{LB} - \widehat{V}_{LC} = a^2hZ_{L1}\widehat{I}_{L1} + a^2\widehat{V}_{F1} - a^2\widehat{V}_{F2} - a^2hZ_{L1}\widehat{I}_{L2} - ahZ_{L1}\widehat{I}_{L1} - a\widehat{V}_{F1} + a\widehat{V}_{F2} + ahZ_{L1}\widehat{I}_{L2}. \tag{3.49}$$

$$\widehat{V}_{LBCT} = (a^2 - a)hZ_{L1}\widehat{I}_{L1} + (a - a^2)hZ_{L1}\widehat{I}_{L2} + (a^2 - a)\widehat{V}_{F1} + (a - a^2)\widehat{V}_{F2}. \tag{3.50}$$

Knowing that:

$$\widehat{I}_{LB} = \hat{I}_{L0} + a^2\hat{I}_{L1} + a\hat{I}_{L2} \tag{3.51}$$

$$\widehat{I}_{LC} = \hat{I}_{L0} + a\hat{I}_{L1} + a^2\hat{I}_{L2} \tag{3.52}$$

then:

$$\widehat{I}_{LBC} = (a^2 - a)\hat{I}_{L1} + (a - a^2)\hat{I}_{L2} \tag{3.53}$$

Substituting Equation (3.53) into Equation (3.50), we obtain the local voltage $\widehat{V}_{LBCT}$:

$$\widehat{V}_{LBCT} = hZ_{L1}\widehat{I}_{LBC} + (a^2 - a)\widehat{V}_{F1} + (a - a^2)\widehat{V}_{F2} \tag{3.54}$$

- Voltage drop $\widehat{V}_{BCT}$ at remote terminal:

In a similar manner, the BC voltage drop seen by the remote terminal $\widehat{V}_{RBC}$ is calculated. Knowing that:

$$\widehat{V}_{RB} = -Z_{N0}\widehat{I}_{R0} + a^2(1-h)Z_{L1}\widehat{I}_{R1} + a^2\widehat{V}_{F1} - a^2\widehat{V}_{F2} - a^2(1-h)Z_{L1}\widehat{I}_{R2} - a^2Z_{N2}\widehat{I}_{R2} - aZ_{N2}\widehat{I}_{R2}. \tag{3.55}$$

$$\widehat{V}_{RC} = -Z_{N0}\widehat{I}_{R0} + a(1-h)Z_{L1}\widehat{I}_{R1} + a\widehat{V}_{F1} - a\widehat{V}_{F2} - a(1-h)Z_{L1}\widehat{I}_{R2} - aZ_{N2}\widehat{I}_{R2} - a^2Z_{N2}\widehat{I}_{R2}. \tag{3.56}$$

Using the voltage in phase B and C, calculate the voltage drop BC at the remote terminal.

$$\widehat{V}_{RBCT} = (a^2 - a)(1 - h)Z_{L1}\widehat{I}_{R1} + (a - a^2)(1 - h)Z_{L1}\widehat{I}_{R2} + (a^2 - a)\widehat{V}_{F1} + (a - a^2)\widehat{V}_{F2}. \quad (3.57)$$

it is known that:

$$\widehat{I}_{RBC} = (a^2 - a)\hat{I}_{R1} + (a - a^2)\hat{I}_{R2} \quad (3.58)$$

Substituting Equation (3.57) into Equation (3.58), we obtain the remote voltage $\widehat{V}_{RBCT}$:

$$\widehat{V}_{RBCT} = (1 - h)Z_{L1}\widehat{I}_{RBC} + (a^2 - a)\widehat{V}_{F1} + (a - a^2)\widehat{V}_{F2} \quad (3.59)$$

Given the voltage drop $\widehat{V}_{BCT}$ at the local and remote terminals, subtract $\widehat{V}_{LBC}$ from $\widehat{V}_{RBC}$.

$$\widehat{V}_{LBCT} - \widehat{V}_{RBCT} = hZ_{L1}\hat{I}_{LBC} + hZ_{L1}\hat{I}_{RBC} - Z_{L1}\hat{I}_{RBC} = hZ_{L1}(\hat{I}_{LBC} + \hat{I}_{RBC}) - Z_{L1}\hat{I}_{RBC} \quad (3.60)$$

Naming the portion $\hat{I}_{LBCT} + \hat{I}_{RBCT}$ of $\hat{I}_{Dif,BCT,2T\phi}$ and isolating the variable h we have:

$$H_{LBCT} = \frac{(\widehat{V}_{LBCT} - \widehat{V}_{RBCT}) + Z_{L1}\hat{I}_{RBC}}{Z_{L1}\hat{I}_{Dif,BCG,2T\phi}} \quad (3.61)$$

3.1.1.4 Single-Line-to-Ground (SLG) Faults

Figure 3.4 illustrates a case of a single-phase fault in phase A at point F of the line. In this type of short, all sequence components are present, as it is an unbalanced fault involving the ground.

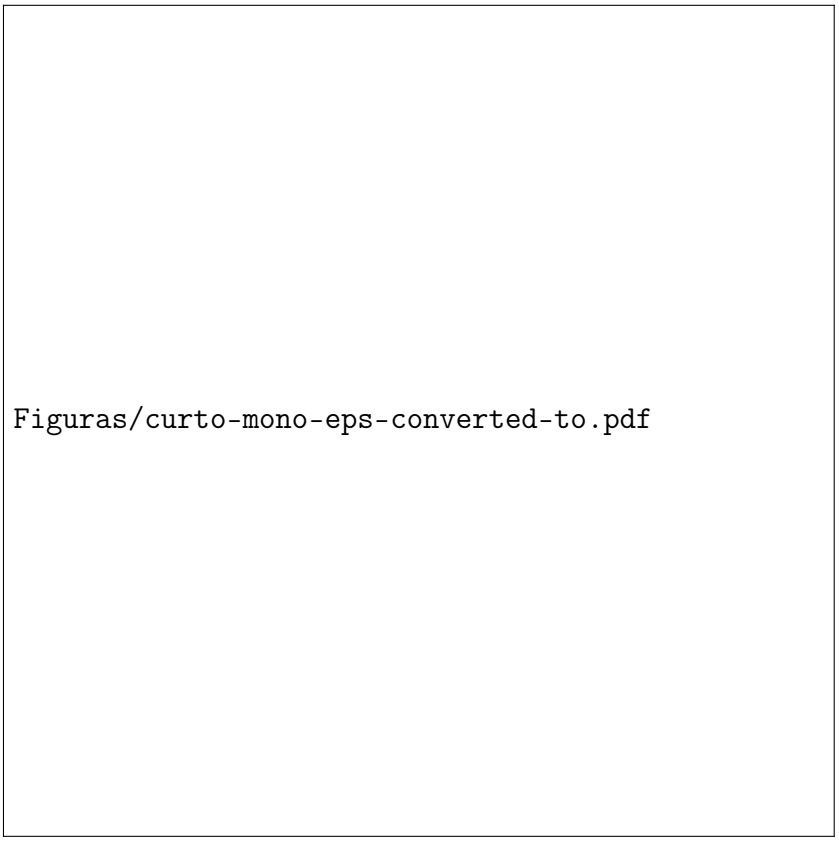

Figure 3.4. Sequence networks for an AG fault.

.

- Voltage $\widehat{V}_A$ at local terminal:

The A-phase voltage seen by the relay at both local and remote terminals are obtained as follow:

$$\widehat{V}_{LA} = \widehat{V}_{L0} + \widehat{V}_{L1} + \widehat{V}_{L2} \tag{3.62}$$

From the circuit illustrated in Figure 3.4

$$\widehat{V}_M = (Z_{M0} + hZ_{L0})\widehat{I}_{L0} + Z_{M1}\widehat{I}_{L1} + Z_{M2}\widehat{I}_{L2} + hZ_{L1}(\widehat{I}_{L1} + \widehat{I}_{L2}) + 3Z_F I_F \tag{3.63}$$

$$\widehat{V}_{L0} = -Z_{M0}\hat{I}_{L0} \tag{3.64}$$

$$\widehat{V}_{L1} = \widehat{V}_M - Z_{M1}\hat{I}_{L1} = (Z_{M0} + hZ_{L0})\hat{I}_{L0} + Z_{M2})\hat{I}_{L2} + hZ_{L1}(\widehat{I}_{L1} + \widehat{I}_{L2}) + 3Z_F I_F \tag{3.65}$$

$$\widehat{V}_{L2} = -Z_{M2}\hat{I}_{L2} \tag{3.66}$$

Substituting Equations (3.64) to (3.66) into (3.62), we obtain $\widehat{V}_{LA}$:

$$\widehat{V}_{LA} = hZ_{L0}\hat{I}_{L0} + hZ_{L1}(\widehat{I}_{L1} + \widehat{I}_{L2}) + 3Z_F I_F \tag{3.67}$$

The phase A current seen by the relay at the Local terminal is given by:

$$\hat{I}_{LA} = \hat{I}_{L0} + \hat{I}_{L1} + \hat{I}_{L2} \tag{3.68}$$

isolating $\hat{I}_{L1} + \hat{I}_{L2}$

$$\hat{I}_{L1} + \hat{I}_{L2} = \hat{I}_{LA} - \hat{I}_{L0} \tag{3.69}$$

Substituting Equation (3.69) in Equation (3.67) and making the appropriate manipulations we get:

$$\widehat{V}_{LA} = hZ_{L1}[(\frac{Z_{L0} - Z_{L1}}{Z_{L1}})\widehat{I}_{L0} + \widehat{I}_{LA}] + 3Z_F I_F \tag{3.70}$$

where $\widehat{I}_{LN} = 3\widehat{I}_{L0}$.

$$\widehat{V}_{LA} = hZ_{L1}[(\frac{Z_{L0} - Z_{L1}}{3Z_{L1}})\widehat{I}_{LN} + \widehat{I}_{LA}] + 3Z_F I_F \tag{3.71}$$

The term $[(\frac{Z_{L0}-Z_{L1}}{3Z_{L1}})\widehat{I}_{LN} + \widehat{I}_{LA}]$ is called $\widehat{I}_{LAcomp}$, get at the voltage seen by the relay in phase A of the Local terminal.

$$\widehat{V}_{LA} = hZ_{L1}\widehat{I}_{LAcomp} + 3Z_F I_F \tag{3.72}$$

- Voltage $\widehat{V}_A$ at remote terminal:

In a similar way to what was done at the Local terminal, all manipulation of the equations originating from the circuit illustrated in Figure 3.4 is done for the remote terminal, thus arriving at the remote voltage seen by the relay in phase A.

$$\widehat{V}_{RA} = (1-h)Z_{L0}\hat{I}_{R0} + (1-h)Z_{L1}(\widehat{I}_{R1} + \widehat{I}_{R2}) + 3Z_F I_F. \tag{3.73}$$

The phase A current seen by the relay at the remote terminal is given by:

$$\hat{I}_{RA} = \hat{I}_{R0} + \hat{I}_{R1} + \hat{I}_{R2} \tag{3.74}$$

isolating the term $\hat{I}_{R1} + \hat{I}_{R2}$

$$\hat{I}_{R1} + \hat{I}_{R2} = \hat{I}_{RA} - \hat{I}_{R0} \tag{3.75}$$

Substituting Equation (3.75) in Equation (3.73) and making the appropriate manipulations we get:

$$\widehat{V}_{RA} = (1-h)Z_{L1}[(\frac{Z_{L0} - Z_{L1}}{Z_{L1}})\widehat{I}_{R0} + \widehat{I}_{RA}] + 3Z_F I_F \tag{3.76}$$

where $\widehat{I}_{RN} = 3\widehat{I}_{R0}$

$$\widehat{V}_{RA} = (1-h)Z_{L1}[(\frac{Z_{L0} - Z_{L1}}{3Z_{L1}})\widehat{I}_{RN} + \widehat{I}_{RA}] + 3Z_F I_F \tag{3.77}$$

Calling the term $[(\frac{Z_{L0}-Z_{L1}}{3Z_{L1}})\widehat{I}_{RN}+\widehat{I}_{RA}]$ as $\widehat{I}_{RAcomp}$, we arrive at the voltage seen by the relay in phase A of the Remote terminal.

$$\widehat{V}_{RA} = (1-h)Z_{L1}\widehat{I}_{RAcomp} + 3Z_F I_F \tag{3.78}$$

With the local and remote voltage values in phase A seen by the relay, subtract $\widehat{V}_{LA} - \widehat{V}_{RA}$ in order to isolate the variable of interest h

$$\widehat{V}_{LA} - \widehat{V}_{RA} = hZ_{L1}\hat{I}_{LAcomp} + hZ_{L1}\hat{I}_{RAcomp} - Z_{L1}\hat{I}_{RAcomp} = hZ_{L1}(\hat{I}_{LAcomp} + \hat{I}_{RAcomp}) - Z_{L1}\hat{I}_{RAcomp} \tag{3.79}$$

The portion $\hat{I}_{LAcomp} + \hat{I}_{RAcomp}$ is called $\hat{I}_{Dif,AT,1\phi}$, the variable h is isolated, thus obtaining the coefficient H for the Fault AG:

$$H_{LAT} = \frac{(\widehat{V}_{LA} - \widehat{V}_{RA}) + Z_{L1}\hat{I}_{RAcomp}}{Z_{L1}\hat{I}_{Dif,AG,1\phi}} \tag{3.80}$$

3.1.2 General Expressions for H_L and H_R

The general expressions for the coefficients H_L and H_R can be written in function of loop voltages and currents as:

$$H_L = \frac{\left(\widehat{V}_{L,loop} - \widehat{V}_{R,loop}\right) + Z_{L1}\hat{I}_{R,loop}}{Z_{L1}\left(\widehat{I}_{L,loop} + \widehat{I}_{R,loop}\right)} \tag{3.81}$$

$$H_R = \frac{\left(\widehat{V}_{R,loop} - \widehat{V}_{L,loop}\right) + Z_{L1}\hat{I}_{L,loop}}{Z_{L1}\left(\widehat{I}_{L,loop} + \widehat{I}_{R,loop}\right)} \tag{3.82}$$

where the loop voltages and currents are chosen depending on the faulted phases (i.e, in accordance with the fault loop), as described in Tab.3.1.

Table 3.1. Loop voltages and currents depending on the faulted phases.

Faulted Phases	$\widehat{V}_{L,loop}$	$\widehat{V}_{R,loop}$	$\widehat{I}_{L,loop}$	$\widehat{I}_{R,loop}$
AG	$\widehat{V}_{LA}$	$\widehat{V}_{RA}$	$\widehat{I}_{LA}$	$\widehat{I}_{RA}$
BG	$\widehat{V}_{LB}$	$\widehat{V}_{RB}$	$\widehat{I}_{LB}$	$\widehat{I}_{RB}$
CG	$\widehat{V}_{LC}$	$\widehat{V}_{RC}$	$\widehat{I}_{LC}$	$\widehat{I}_{RC}$
AB	$\widehat{V}_{LA}$ - $\widehat{V}_{LB}$	$\widehat{V}_{RA}$ - $\widehat{V}_{RB}$	$\widehat{I}_{LA}$- $\widehat{I}_{LB}$	$\widehat{I}_{RA}$- $\widehat{I}_{RB}$
BC	$\widehat{V}_{LB}$ - $\widehat{V}_{LC}$	$\widehat{V}_{RB}$ - $\widehat{V}_{RC}$	$\widehat{I}_{LB}$- $\widehat{I}_{LC}$	$\widehat{I}_{RB}$- $\widehat{I}_{RC}$
CA	$\widehat{V}_{LC}$ - $\widehat{V}_{LA}$	$\widehat{V}_{RC}$ - $\widehat{V}_{RA}$	$\widehat{I}_{LC}$- $\widehat{I}_{LA}$	$\widehat{I}_{RC}$- $\widehat{I}_{RA}$
ABC	$\widehat{V}_{LA}$ - $\widehat{V}_{LB}$	$\widehat{V}_{RA}$ - $\widehat{V}_{RB}$	$\widehat{I}_{LA}$- $\widehat{I}_{LB}$	$\widehat{I}_{RA}$- $\widehat{I}_{RB}$

Having made all the equations for the calculation of H_L and H_R for all types of faults, the following is a detailed description of the proposed algorithm.

3.2 PHASE CURRENTS COMPENSATION

The proposed algorithm employs phase current compensation in each line terminal, by removing the line charging current and the shunt reactor current, if any. For the sake of simplicity, it is presented here the formulation for the local terminal only.

The line charge current per phase is computed for the local terminal as follows:

$$\begin{bmatrix} \widehat{I}_{LA,cap} \\ \widehat{I}_{LB,cap} \\ \widehat{I}_{LC,cap} \end{bmatrix} = j\frac{\omega}{2} \begin{bmatrix} C_p & C_m & C_m \\ C_m & C_p & C_m \\ C_m & C_m & C_p \end{bmatrix} . \begin{bmatrix} \widehat{V}_{LA} \\ \widehat{V}_{LB} \\ \widehat{V}_{LC} \end{bmatrix} \tag{3.83}$$

where C_p and C_m are the self and mutual shunt capacitance of the transmission line, respectively. On the other hand, for the local terminal, the shunt reactor current, if any, can be computed as:

$$\widehat{I}_{L\phi,ind} = \frac{\widehat{V}_{L\phi}}{Z_{ind}}, \tag{3.84}$$

where Z_{ind} is the per phase impedance of the shunt reactor, and ϕ stands for phases A, B or C. Thereby, the phase compensated currents for local terminal are obtained as:

$$\widehat{I}_{L\phi X} = \widehat{I}_{L\phi} - \widehat{I}_{L\phi,cap} - \widehat{I}_{L\phi,ind} \tag{3.85}$$

Likewise, one can obtain the line charging currents $\widehat{I}_{R\phi,cap}$ and shunt reactor currents $\widehat{I}_{R\phi,ind}$ for the remote terminal, as well as the phase compensated currents $\widehat{I}_{R\phi X}$.

3.3 FAULTED PHASE SELECTION

As aforementioned, the proposed algorithm relies on faulted phases selection to single out the correct loop voltages and currents (described in na Tab. 3.1) to calculate H_L and H_R properly. To do so, the proposed algorithm is based on the current differential protection principle, such that it evaluates the operating current computed per phase as:

$$\widehat{I}_{op\phi} = |\widehat{I}_{L\phi X} + \widehat{I}_{R\phi X}| \tag{3.86}$$

Basically, if $I_{op\phi} \geq I_{min}$, where I_{min} is a pick-up threshold, phase ϕ is selected as a faulted phase.

3.4 COEFFICIENTS Γ

Aiming to evaluate trip command issuing, the coefficients Γ_L and Γ_R for local and remote line terminals, respectively, are calculated as follows:

$$\Gamma_L = \frac{1 + H_L}{1 + F_{ext} \cdot K_{harmT} \cdot \dfrac{I_{harmT}}{|\widehat{I}_{L,loop} + \widehat{I}_{R,loop}|}} \tag{3.87}$$

$$\Gamma_R = \frac{1 + H_R}{1 + F_{ext} \cdot K_{harmT} \cdot \dfrac{I_{harmT}}{|\widehat{I}_{L,loop} + \widehat{I}_{R,loop}|}} \tag{3.88}$$

where currents $\widehat{I}_{L,loop}$ and $\widehat{I}_{R,loop}$ are chosen according to Tab.3.1; F_{ext} is the external fault declaration (a boolean value set either 1 or 0); K_{harmT} is a sensitivity parameter; and I_{harmT} is the total harmonic restraint

The purpose of this trip variable is to make the algorithm more robust to possible errors in estimating the location of the fault (H_L and H_R). Therefore, the numerator of the equation will prevail in the case of an internal fault (1 + Γ), thus taking the variable outside the restriction characteristic. In the case of an external fault, the variable Fext is equal to 1, and when the CT is saturated, the denominator of the equation increases in value in order to take the variables Γ_L and Γ_R to a value less than one, thus ensuring that this variable remains within the restriction characteristic, not sending a trip command.

I_{harmT} is the total harmonic restraint current computed as:

$$I_{harmT} = |\widehat{I}_{L,2h}| + |\widehat{I}_{R,2h}| + |\widehat{I}_{L,3h}| + |\widehat{I}_{R,3h}| + |\widehat{I}_{L,4h}| + |\widehat{I}_{R,4h}| \tag{3.89}$$

with subscripts 2h, 3h and 4h standing for the 2^{o}, 3^{o} and 4^{o} harmonic components, respectively.

3.5 RESTRAINT CHARACTERISTIC

Coefficients Γ_L and Γ_R are understood based on the graphical representation, in which the abscissa and ordinate axes correspond to their real and imaginary parts, as presented in Fig. 3.5. The proposed restraint region is defined by a circle with a unit radius and center at the origin. In a normal operating condition, the coefficient is fixed at (0,0). In case of an external fault, the coefficients might leave the stability point (0,0), but remain within the restraint characteristic. Conversely, if an internal fault takes place, at least Γ_L or Γ_R moves toward outside the restraint region.

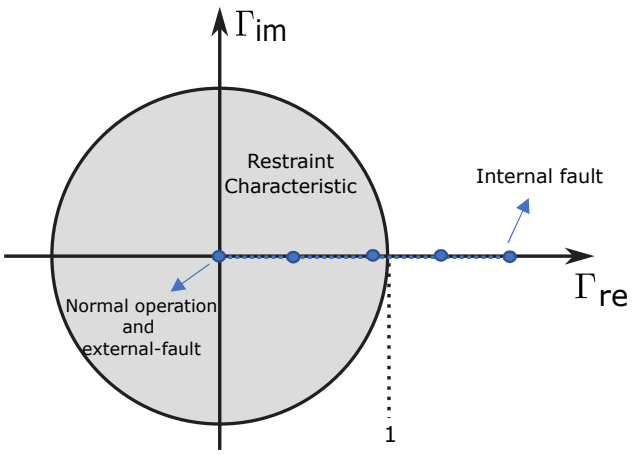

Figure 3.5. Proposed restraint characteristic.

.

It is worth noting that although the Figure 3.5 shows the displacement of Γ exactly above the real axis, this is not the behavior of the variable, it will leave the characteristic with different behaviors.

3.6 OVERALL DESCRIPTION

Figure 3.6 illustrates the block diagram of the proposed algorithm. In this scheme, the indices L and R correspond to the signals from the local and remote terminals, respectively, and φ represents phase A, B or C. The blocks presented and their functionalities are described in detail in the subsequent sections.

3.6.1 Signal Acquisition

The `Signal Acquisition` block is used to acquire secondary current and voltage signals from CTs and voltage transformers (VTs) using two different sampling rates: 256 samples per cycle (HSR - high sampling rate) this rate is used exclusively in the external fault detection algorithm as there are derivative calculations that require a higher rate to perform successfully and 16 samples per cycle (LSR - low sampling rate)

3.6.2 Signal Alignment and Scaling

The `Signal Alignment and Scaling` block scales up HSR and LSR signals from the secondary to primary values of CTs and VTs, besides carrying out the signals alignment to get rid off time difference between samples from local and remote line terminals.

3.6.3 Phasor Estimation

The `Phasor Estimation` block is applied to calculate voltage and current fundamental phasors, as well as the $2^{\underline{a}}$, $3^{\underline{a}}$ and $4^{\underline{a}}$ harmonic components of current signals. In the present work, the Modified Cosine Filter reported in (HART et al., 2000) was implemented, due to its simplicity and good removal of the exponentially decaying component.

3.6.4 External Fault Detection

The External Fault Detection block determines whether the occurrence verified is internal or external to the protected transmission line, with the aim of increasing protection security in situations of external short circuits that lead to possible saturation of the CTs.Use HSR current signals to determine if a fault is external to the protected transmission line, with the aim of increasing the security for external faults that lead to CT saturation. To do so, the instantaneous current-based differential principle is employed (MILLER *et al.*, 2010) and (VASQUEZ; SILVA, 2019) .

3.6.5 Current Compensation

The `Current Compensation` block removes the line charging currents and the shunt reactor currents, if any, from the phase currents.

3.6.6 Faulted Phase Selection

The `Faulted Phase Selection` block uses phasor-based differential principle to select the faulted phases

3.6.7 Calculation of H_L and H_R

Based on the phase selection, it is identified for which Fault Loop the coefficients of H_L and H_R will be calculated .Thereby, H_L and H_R are computed using (3.81) and (3.82), considering the proper variables described in Tab.3.1 depending on the faulted phases.

3.6.8 Calculation of Γ_L and Γ_R

Then Γ_L and Γ_R are computed using (3.87) and (3.88), taking as input: H_L and H_R; the output of the `External Fault Detection` block; the output of the `Phase Selection` block; and the harmonic components obtained in the `Phasor Estimation` block.

3.6.9 Trip Decision

Finally, the `Trip Decision` block issues a trip command whenever Γ_L or Γ_R moves toward outside the restraint characteristic.

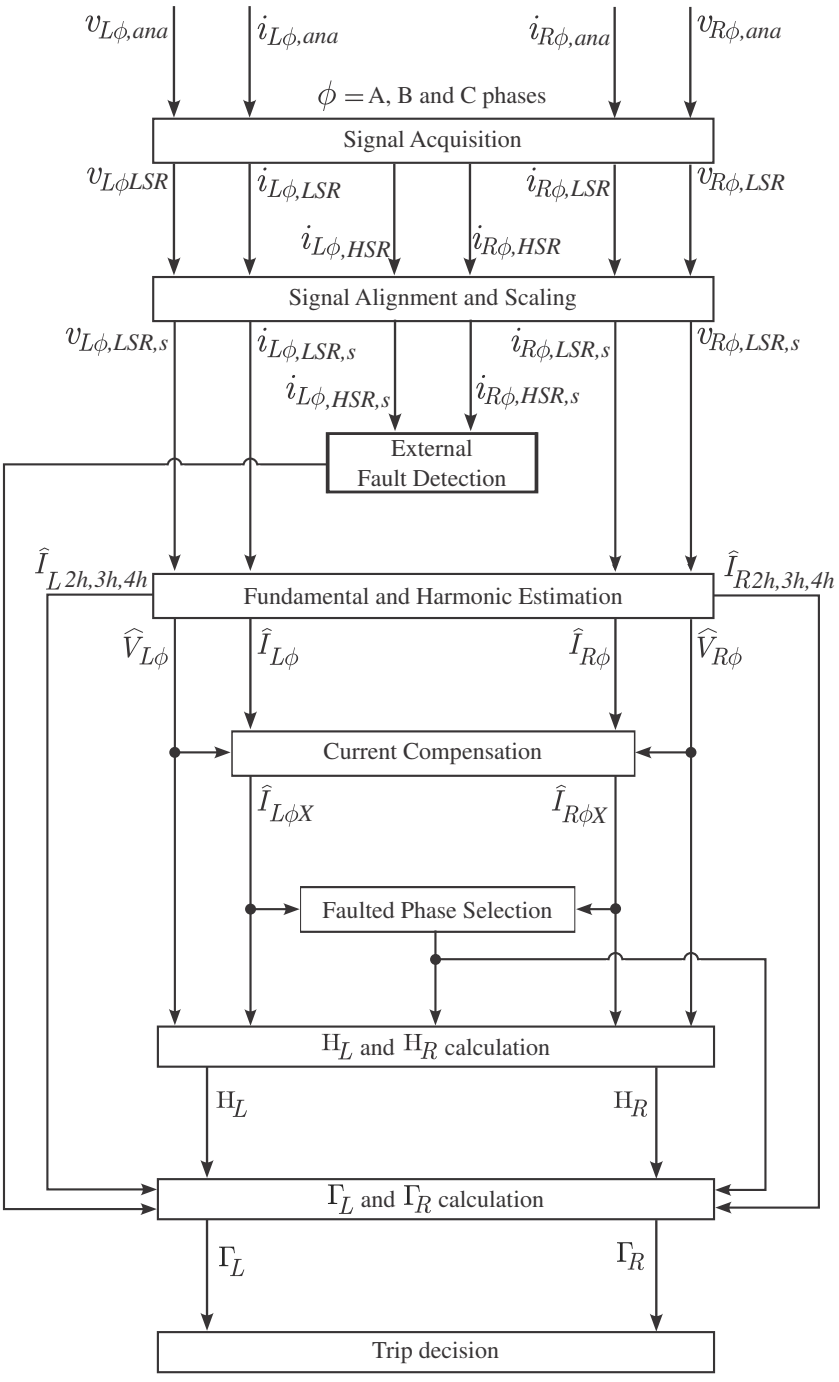

Figure 3.6. Block diagram of the proposed algorithm.

CHAPTER 4

RESULTS

Aiming to evaluate the proposed algorithm, simulations were divided into fault transient and parametric sensitivity analyses. In the first case, it is highlighted the transient performance of the proposed algorithm from the pre-fault to post-fault steady-state condition, whereas the second case leads to a more comprehensive understanding of how the proposed algorithm is sensitive to each fault and system parameter.

4.1 FAULT TRANSIENT ANALYSIS

In order to assess the proposed algorithm transient performance, several faults were simulated using an ATPDraw model the represents a part of Brazilian interconnected power grid, which includes power equipment in the vicinity of the 500 kV double circuit series-compensated line 387 km long, between Imperatriz and Presidente Dutra stations (Figure 4.1). It is a complex part of the system, because it interconnects the North and Northeast Brazilian regions, and concentrates several series-compensated lines, huge power generation plants, HVDC lines, etc

Regarding the ATPDraw model, it has been implemented by the Brazilian power utility Eletronorte considering real data from power equipment, and has been used on electromagnetic transient studies for protection relays factory acceptance tests and commissioning. In Figure 4.2, it is highlighted the ATPDraw model of the evaluated double circuit line. The circuits share the same right-of-way, but not the same tower, and they were implemented using a distributed and frequency-independent parameter model, considering the actual transposition scheme employed in the field (i.e., $1/6 - 1/3 - 1/3 - 1/6$).

The series capacitor banks were modeled with manufacturer data, representing the capacitors, metal-oxide varistors (MOVs), triggered air GAP, current limiting reactor, damping

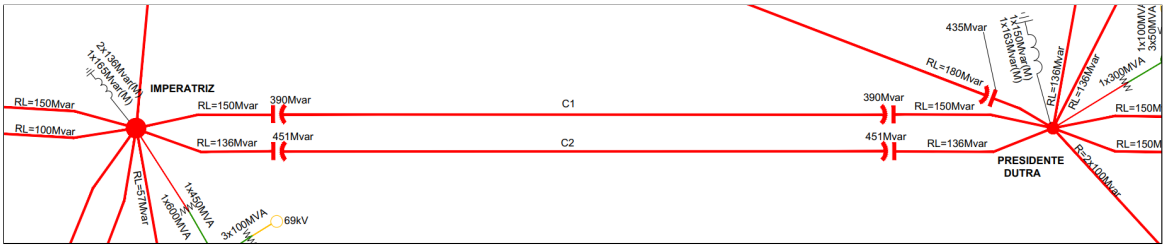

Figure 4.1. Part of the Brazilian power grid, highlighting the 500 kV double circuit series-compensated line between Imperatriz and Presidente Dutra substations.

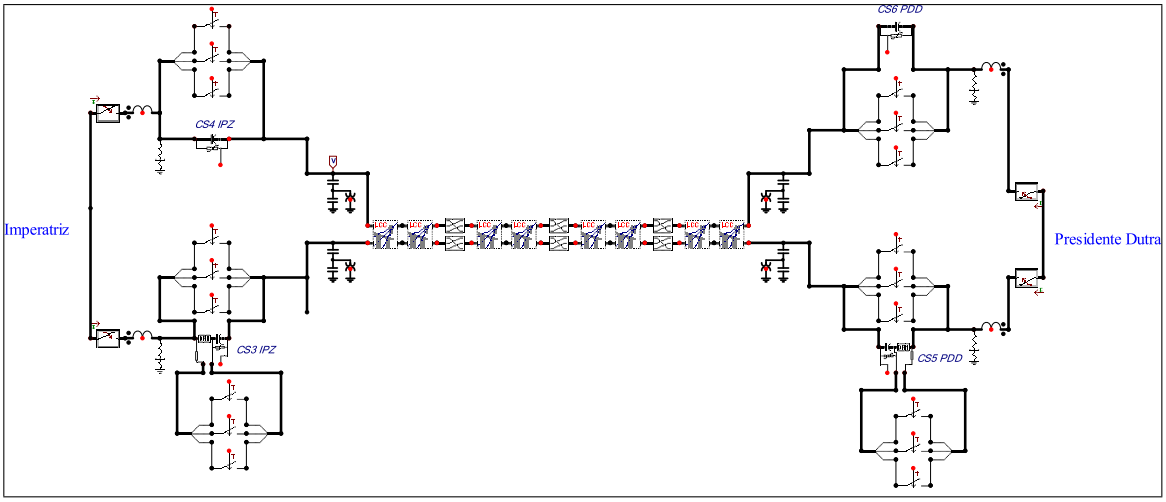

Figure 4.2. ATPDraw model of the 500 kV double circuit series-compensated line between Imperatriz and Presidente Dutra substations.

circuit, etc. The CT and coupling capacitor VT (CCVT) models reported in (IEEE POWER SYSTEM RELAYING COMMITTEE, 2004) and (PAJUELO *et al.*, 2008), respectively, were also included. Therefore, the proposed algorithm could be evaluated by means of quite realistic simulations.

Several fault cases were evaluated, for the sake of space, here the transient performance of the proposed algorithm for six cases are presented. The performance of the conventional alpha plane-based phase differential elements and the adaptive alpha plane-based algorithm reported in (SARANGI; PRADHAN, 2017) were also assessed for the same cases, highlighting the advantages of the proposed algorithm.

4.1.1 Case 1 and Case 2 - Fault Transient Analysis - SGL Faults

In Case 1, it was simulated an internal AG fault at 1% of the line from Imperatriz substation, with 150 Ω of fault resistance. Figures. 4.3 and 4.4 present the local and remote terminals currents and voltages during the fault. In this case, the triggered air GAP of the series capacitor bank of the faulted circuit in Imperatriz station did not operate, so that one can see subsynchronous oscillations on current signals. Figure 4.5 presents the performance of the alpha plane-based local and remote terminals phase differential elements. It can be seen that because of the large fault resistance, these elements are unable to detect the fault (i.e., points still remain inside the restraint characteristic).

In Figure 4.6, the proposed algorithm performance is depicted. It is observed that coefficients Γ_L and Γ_R move outside the restraint characteristic, correctly identifying the fault inside the protected transmission line. It reveals that the proposed algorithm provides more sensitivity than the conventional alpha plane-based phase differential elements for this case.

In Figure 4.7, it is shown the binary status of the trip command from the proposed algorithm, the conventional alpha plane-based differential protection algorithm, and the adaptive alpha plane-based algorithm reported in (SARANGI; PRADHAN, 2017). It is observed that, in this case, the coefficient Γ_R operates correctly on detecting the fault, whereas the coefficient Γ_L detects the fault during just a period of time. It occurs because Γ_L moves towards outside the restraint region, but return to inside it. Nevertheless, since a trip command is issued whenever Γ_L or Γ_R moves outside the restraint region, the proposed algorithm still provide a correct operation. Conversely, the other evaluated protection elements were not able to detect the fault.

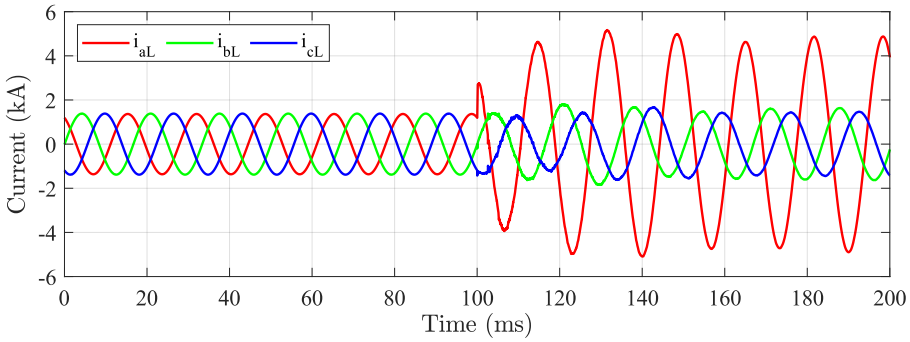

(a) Currents

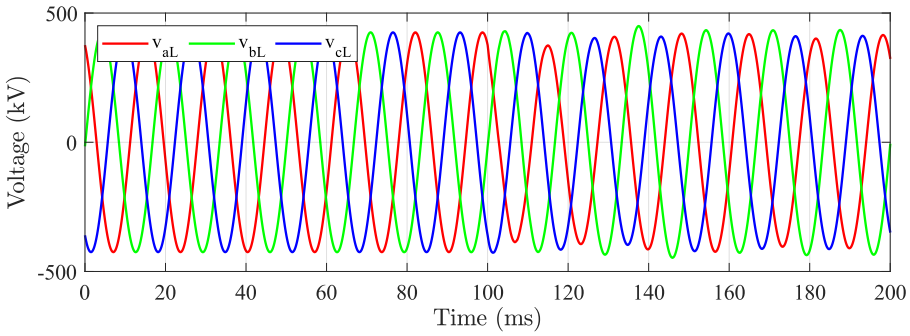

(b) Voltages

Figure 4.3. Case 1 - Local currents and voltages for an internal AG fault at 1% of the transmission line.

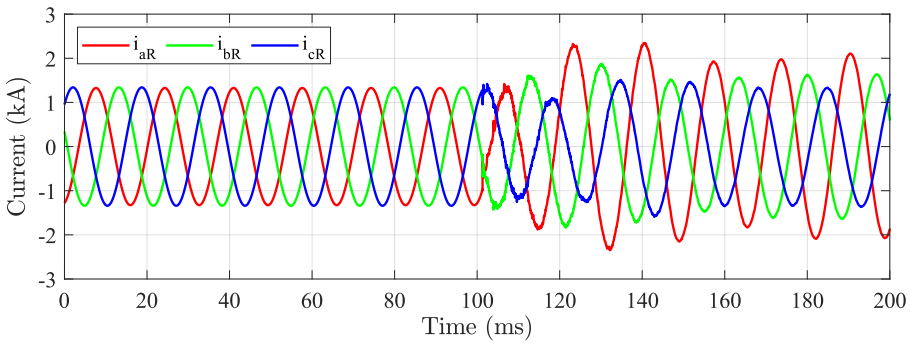

(a) Currents

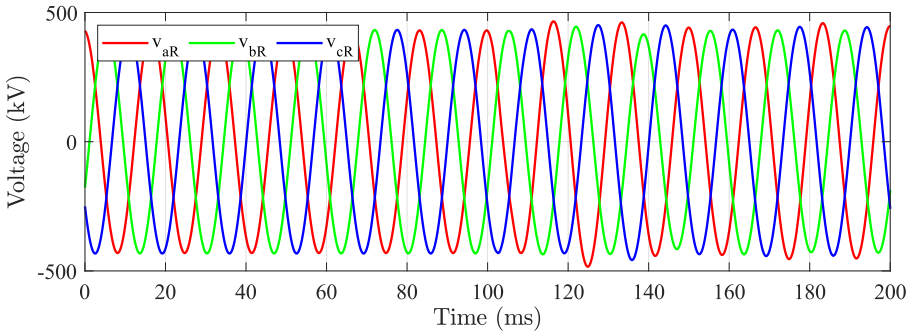

(b) Voltages

Figure 4.4. Case 1 - Remote currents and voltages for an internal AG fault at 1% of the transmission line.

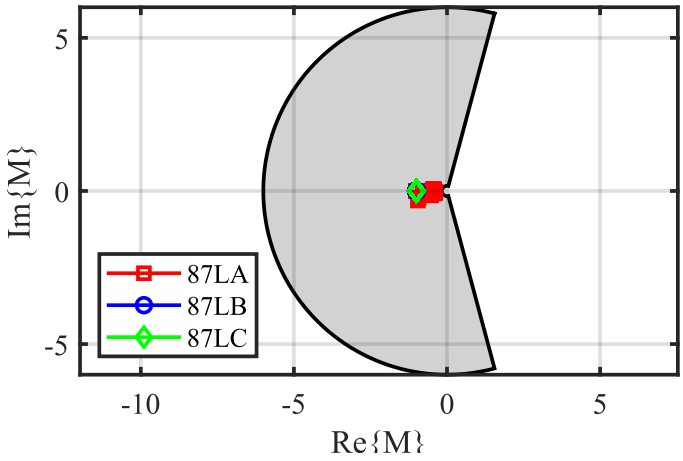

(a) Local terminal

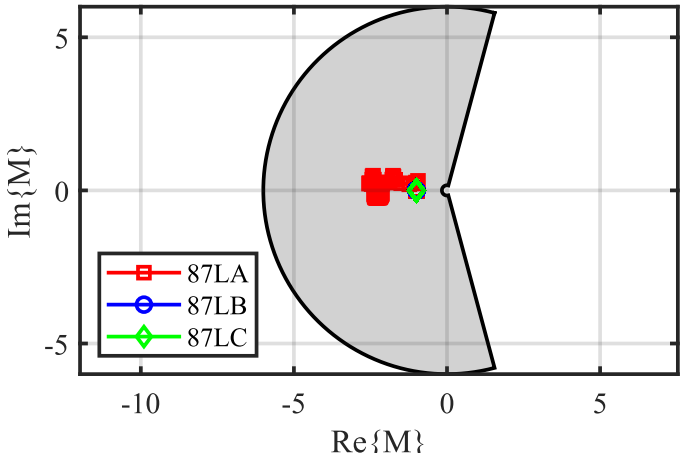

(b) Remote terminal

Figure 4.5. Case 1 - Alpha plane-based phase differential elements.

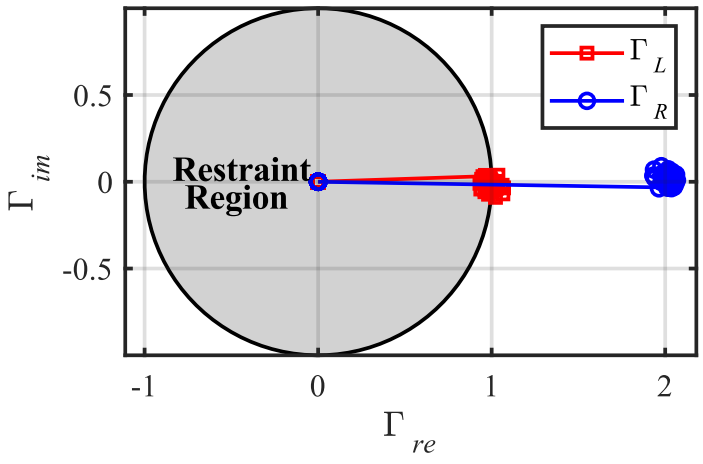

Figure 4.6. Case 1 - Proposed algorithm.

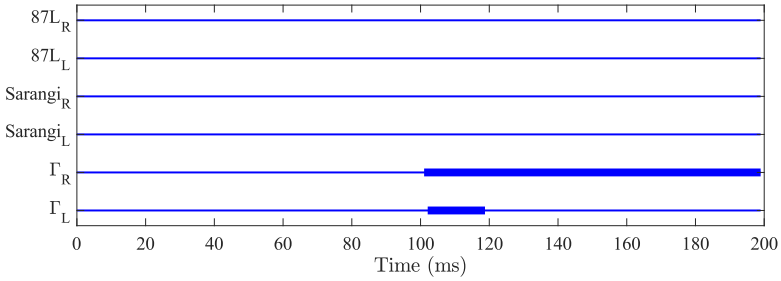

Figure 4.7. Case 1: Algorithms comparison.

In case 2, an internal AG fault was simulated at 129 km of the Imperatriz substation line, with 50 Ω of fault resistance. Figures 4.8 and 4.9 show the currents and voltages of the local and remote terminals during the fault. In this case also, the air gap triggered by the series capacitor bank of the faulted circuit at the Imperatriz station did not operate, so that it is possible to see subsynchronous oscillations in the current signals. Figure 4.10 shows the performance of the phase differential elements of the local and remote terminals based on the alpha plane. It can be observed that in this case these elements are able to detect the fault correctly.

In Figure 4.6, the proposed algorithm performance is depicted. It is observed that coefficients Γ_L and Γ_R move outside the restraint characteristic, correctly identifying the fault inside the protected transmission line.

In Figure4.12 it can be seen that, in this case, the coefficients Γ_R and Γ_L operate correctly in detecting the fault, the other protection elements evaluated also detect the defect but take longer to identify the fault.

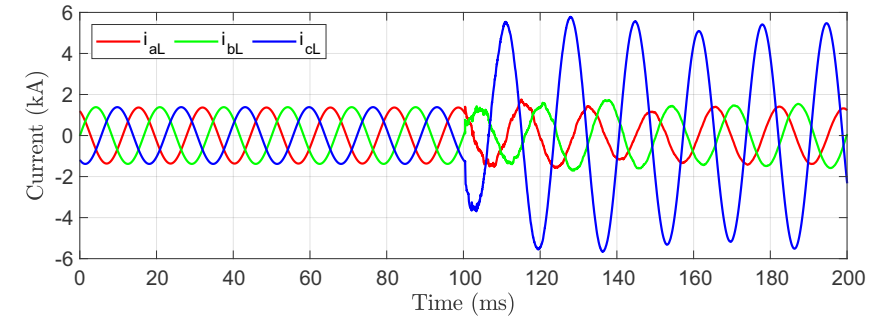

(a) Currents

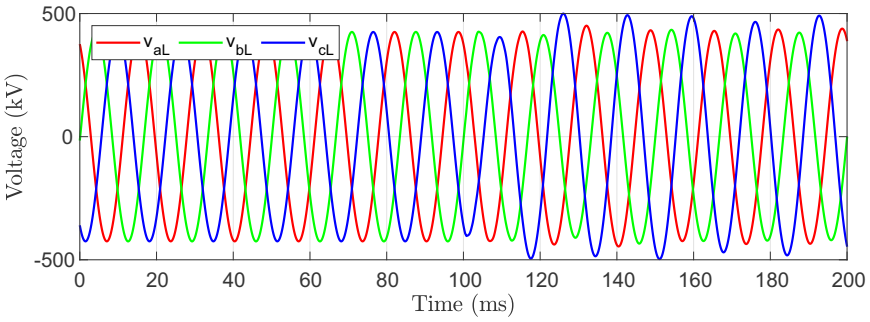

(b) Voltages

Figure 4.8. Case 2 - Local currents and voltages for an internal AG fault at 129km of the transmission line.

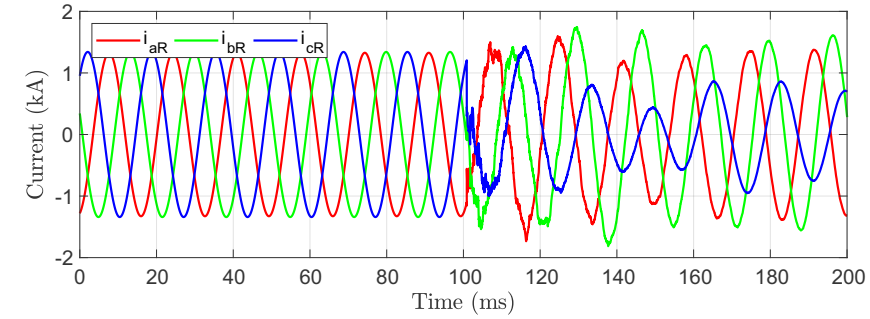

(a) Currents

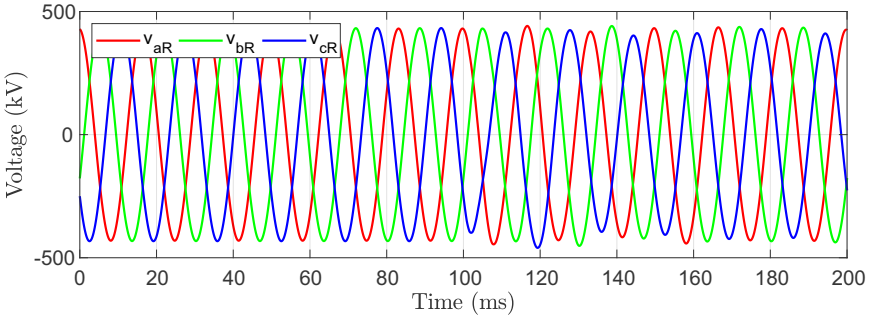

(b) Voltages

Figure 4.9. Case 1 - Remote currents and voltages for an internal AG fault at 129km of the transmission line.

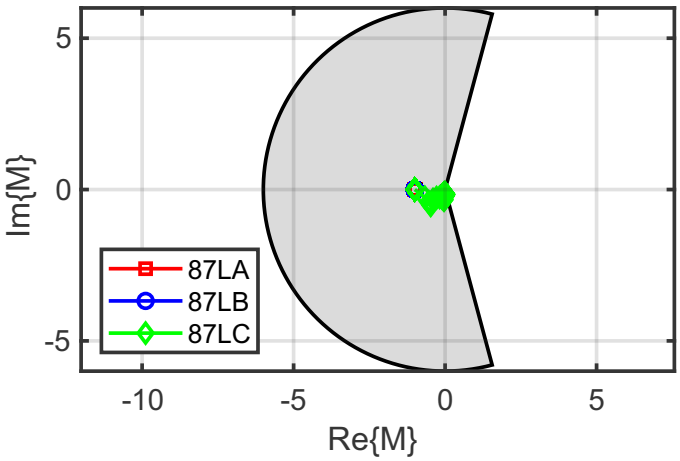

(a) Local terminal

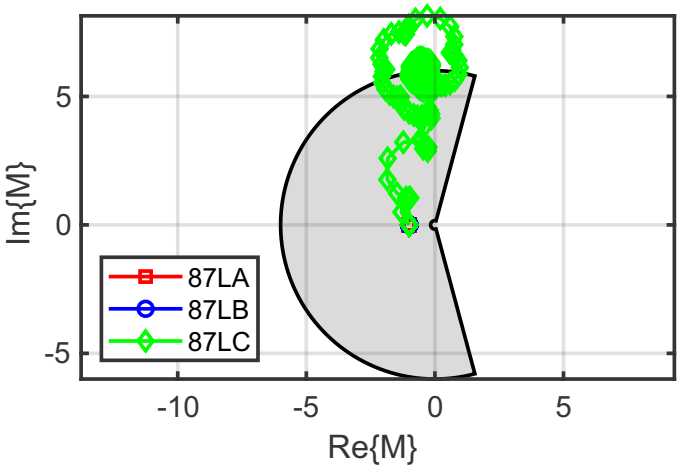

(b) Remote terminal

Figure 4.10. Case 2 - Alpha plane-based phase differential elements.

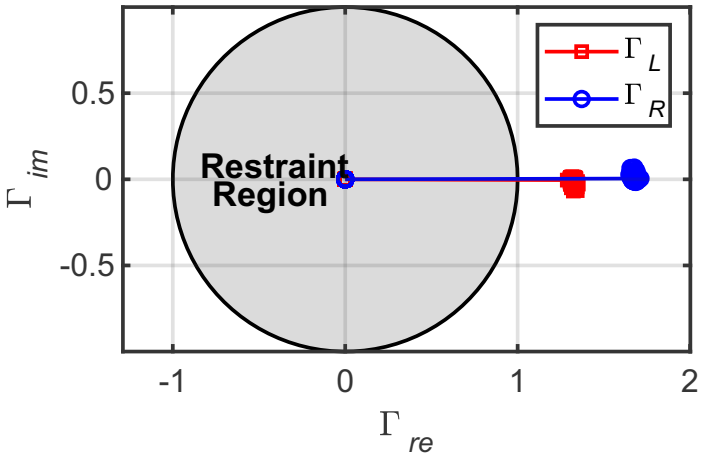

Figure 4.11. Case 2 - Proposed algorithm.

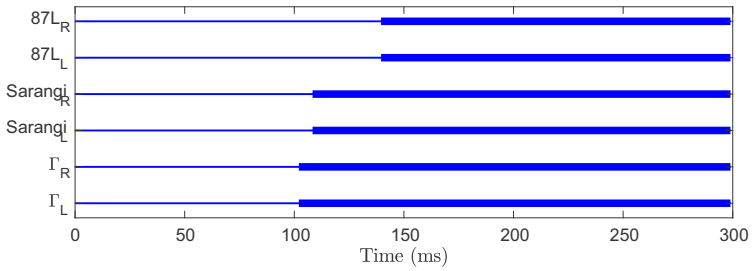

Figure 4.12. Case 2: Algorithms comparison.

4.1.2 Case 3- Fault Transient Analysis - 2P Fault

In this case, an internal BC fault was simulated at 258 km of the Imperatriz substation line, with 0 Ω of fault resistance. Figures 4.13 and 4.14 show the currents and voltages of the local and remote terminals during the fault. Figure 4.15 shows the performance of the phase differential elements of the local and remote terminals based on the alpha plane. It can be observed that these elements are able to detect the fault correctly (i.e., the phase elements leave the restraint characteristic).

In Figure 4.16, the performance of the proposed algorithm is represented. It is observed that the coefficients Γ_L and Γ_R move outside the constraint characteristic, correctly identifying the fault within the protected transmission line.

In Figure 4.17, the binary state of the trip command of the proposed algorithm, the conventional alpha-plane-based differential protection algorithm, and the alpha-plane-based adaptive algorithm reported in (SARANGI; PRADHAN, 2017) are shown. It can be observed that, in this case, the coefficient Γ_L and Γ_R operate correctly in fault detection, thus the other evaluated protection elements were able to detect the fault.

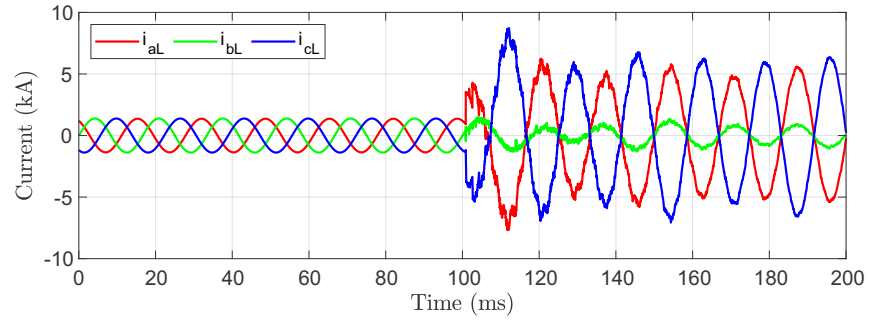

(a) Currents

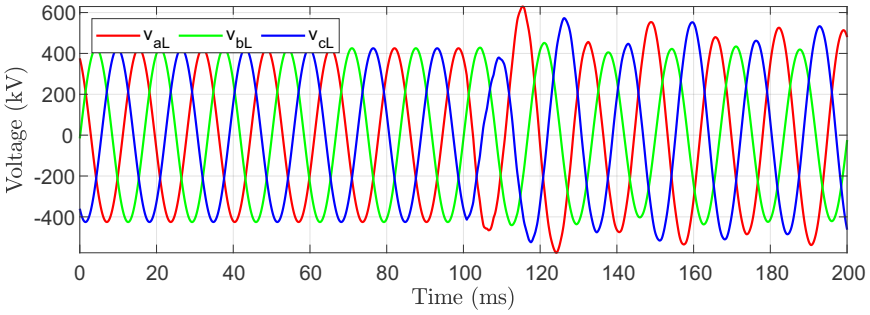

(b) Voltages

Figure 4.13. Case 3 - Local currents and voltages for an internal BC fautl the transmission line.

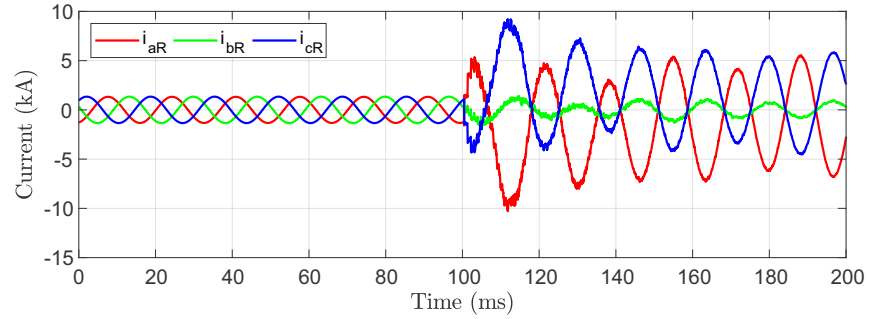

(a) Currents

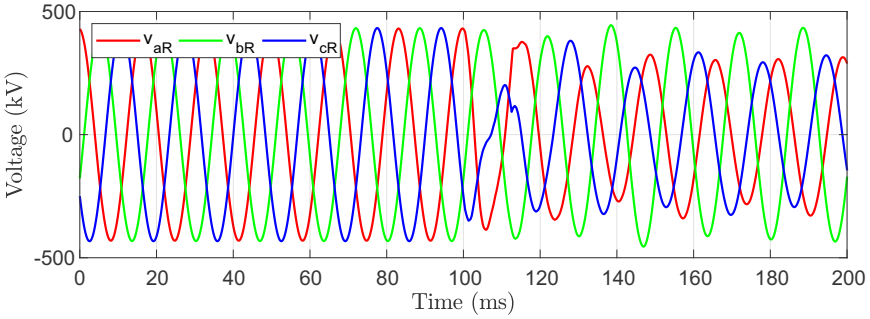

(b) Voltages

Figure 4.14. Case 3 - Remote currents and voltages for an internal BC fault the transmission line.

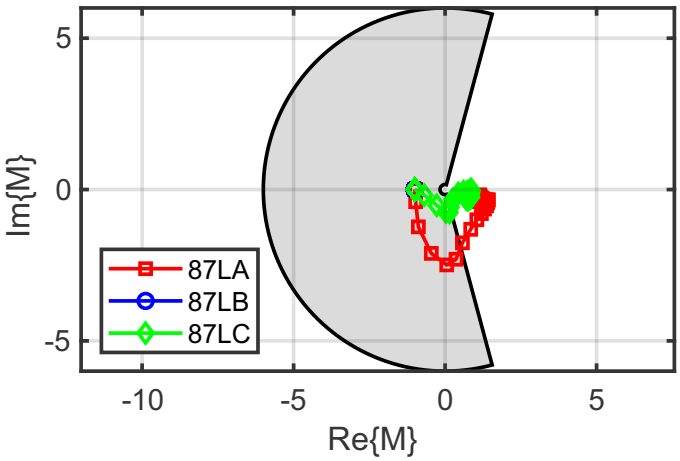

(a) Local terminal

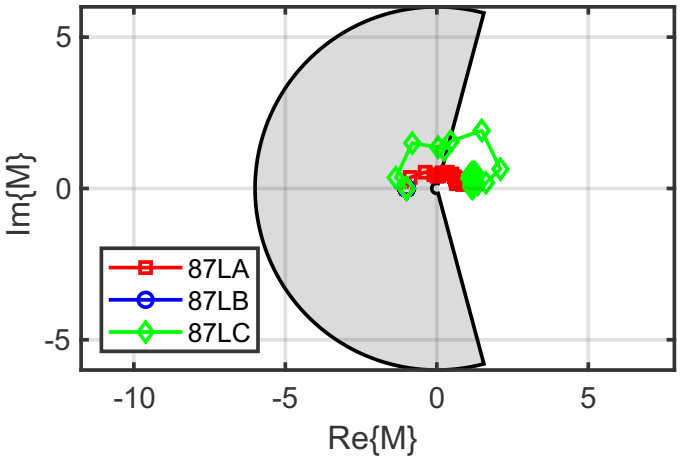

(b) Remote terminal

Figure 4.15. Case 3 - Alpha plane-based phase differential elements.

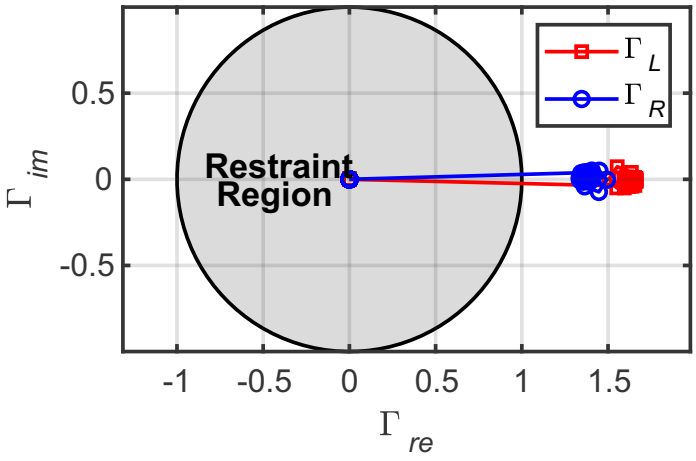

Figure 4.16. Case 3 - Proposed algorithm.

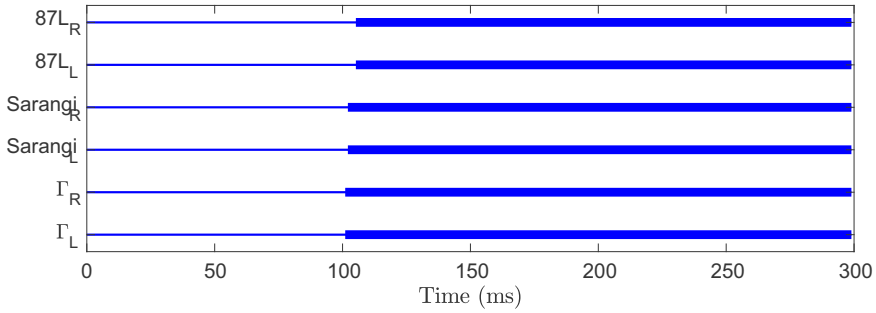

Figure 4.17. Case 3: Algorithms comparison.

4.1.3 Case 4- Fault Transient Analysis - 2PG Fault

In this case, an internal CAG fault was simulated at 354,75 km of the Imperatriz substation line, with 100Ω of fault resistance. Figures 4.18 and 4.19 show the currents and voltages of the local and remote terminals during the fault. Figure 4.20 shows the performance of the phase differential elements of the local and remote terminals based on the alpha plane. It can be observed that these elements are able to detect the fault correctly (i.e., the phase elements leave the restraint characteristic).

In Figure4.21, the performance of the proposed algorithm is represented. It is observed that the coefficients Γ_L and Γ_R move outside the constraint characteristic, correctly identifying the fault within the protected transmission line. In Figure4.22, the binary state of the trip command of the proposed algorithm, the conventional alpha-plane-based differential protection algorithm, and the alpha-plane-based adaptive algorithm reported in (SARANGI; PRADHAN, 2017) are shown. It can be observed that, in this case, the coefficient Γ_L and Γ_R operate correctly in fault detection, thus the other evaluated protection elements were able to detect the fault.

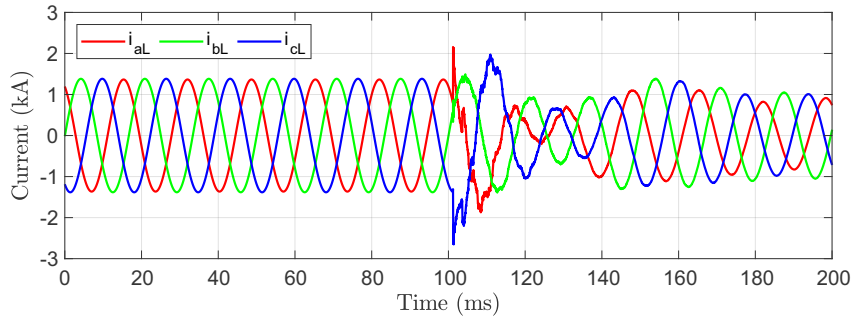

(a) Currents

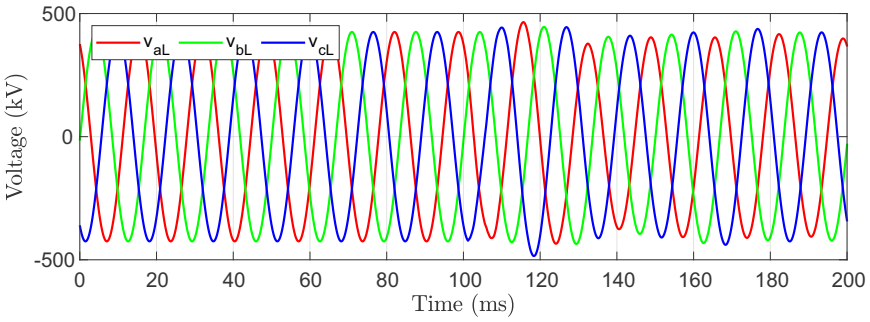

(b) Voltages

Figure 4.18. Case 4 - Local currents and voltages for an internal BC fautl the transmission line.

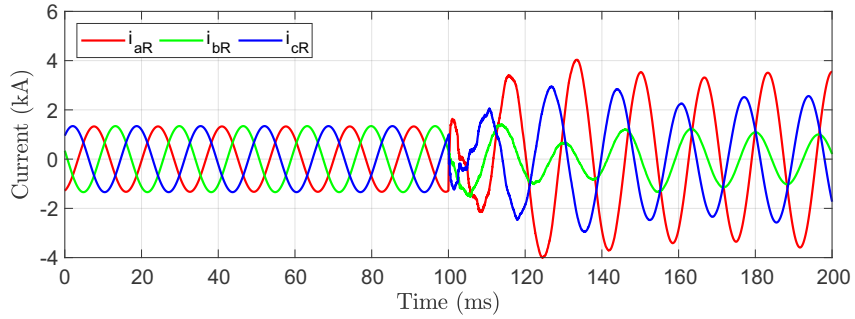

(a) Currents

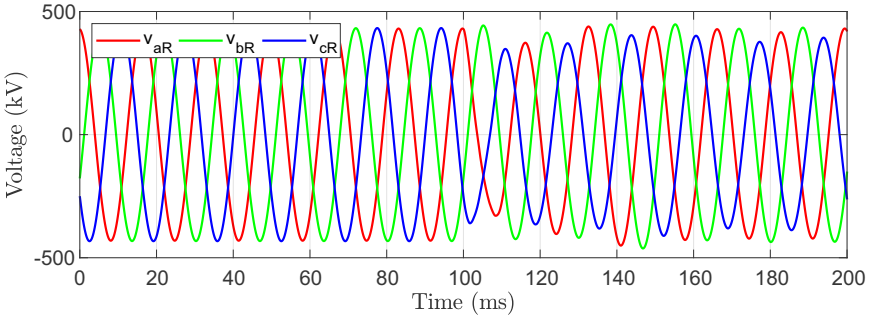

(b) Voltages

Figure 4.19. Case 4 - Remote currents and voltages for an internal CAG fault the transmission line.

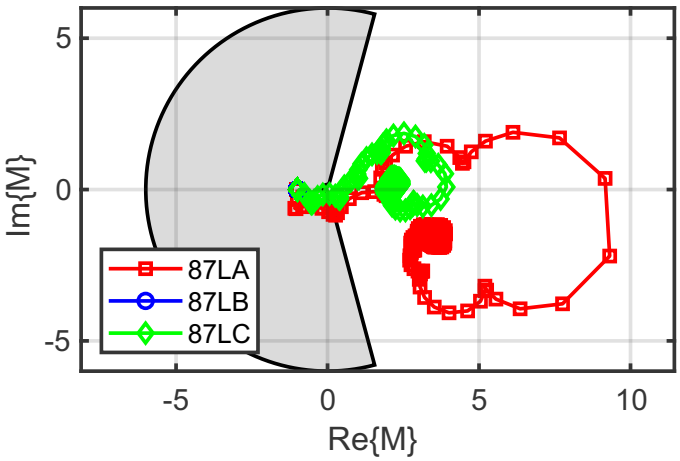

(a) Local terminal

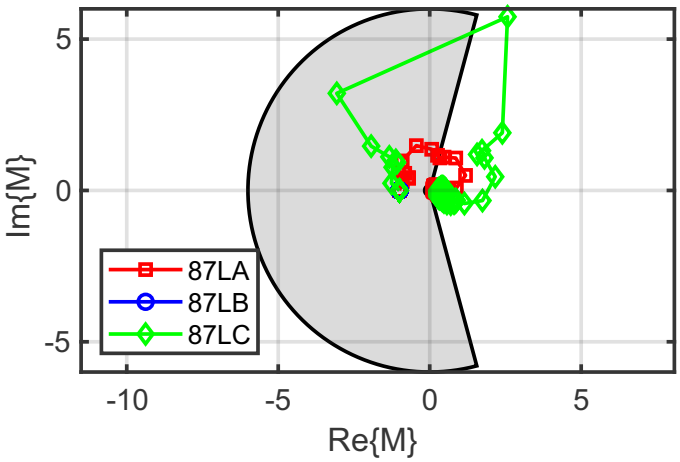

(b) Remote terminal

Figure 4.20. Case 4 - Alpha plane-based phase differential elements.

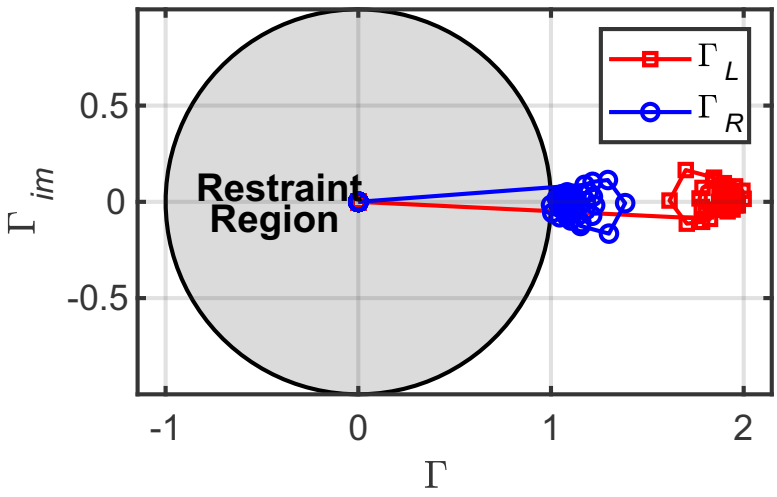

Figure 4.21. Case 4 - Proposed algorithm.

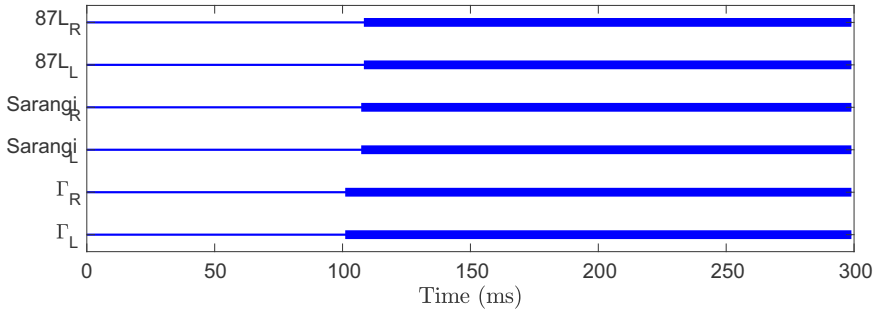

Figure 4.22. Case 4: Algorithms comparison.

4.1.4 Case 5 - Fault Transient Analysis - 3P Fault

In this case, an internal ABC fault was simulated at 0 km of the Imperatriz substation line, with 0 Ω of fault resistance, in which case the local CT was forcibly saturated. Figures 4.23 and 4.24 show the currents and voltages of the local and remote terminals during the fault. Fig. 4.25 shows the performance of the phase differential elements of the local and remote terminals based on the alpha plane. It can be observed that the elements are capable of detecting the fault.

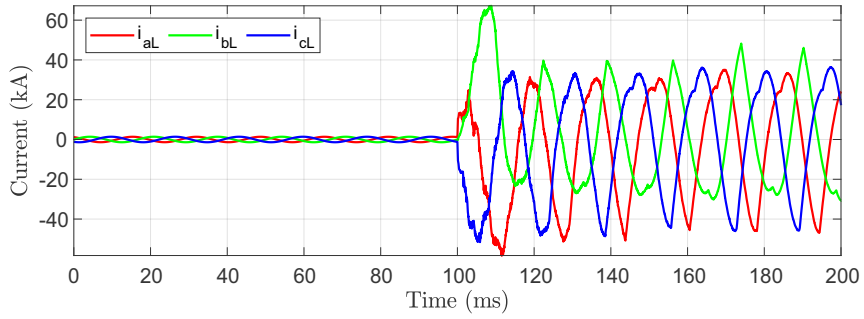

(a) Currents

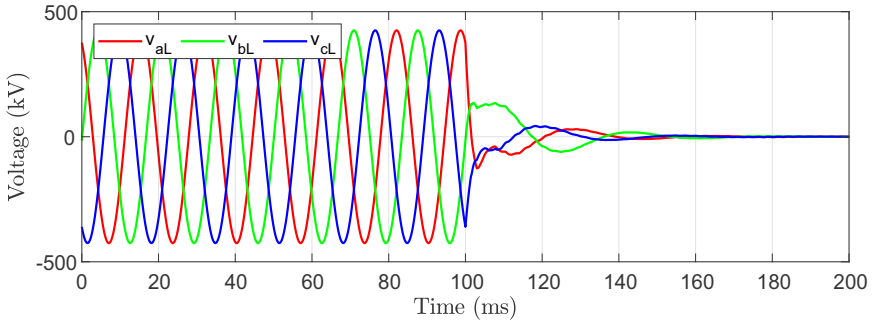

(b) Voltages

Figure 4.23. Case 5 - Local currents and voltages for an internal ABC fautl the transmission line.

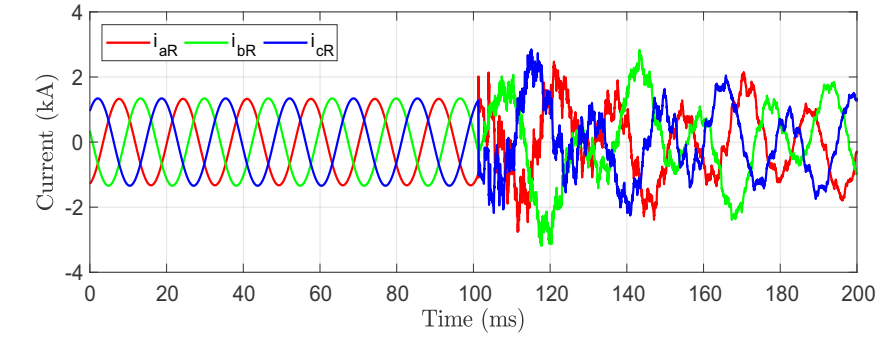

(a) Currents

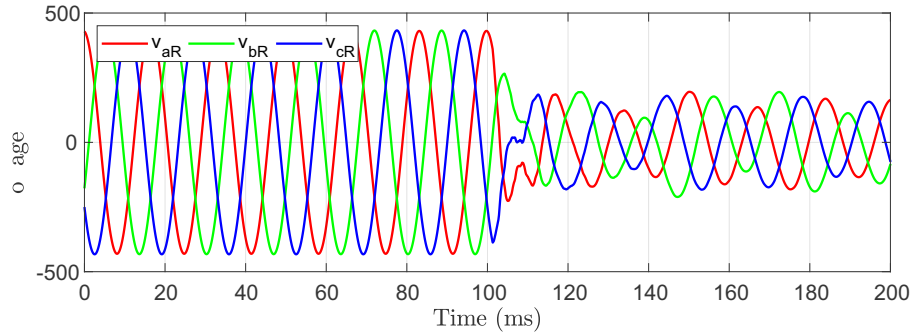

(b) Voltages

Figure 4.24. Case 5 - Remote currents and voltages for an internal ABC fault the transmission line.

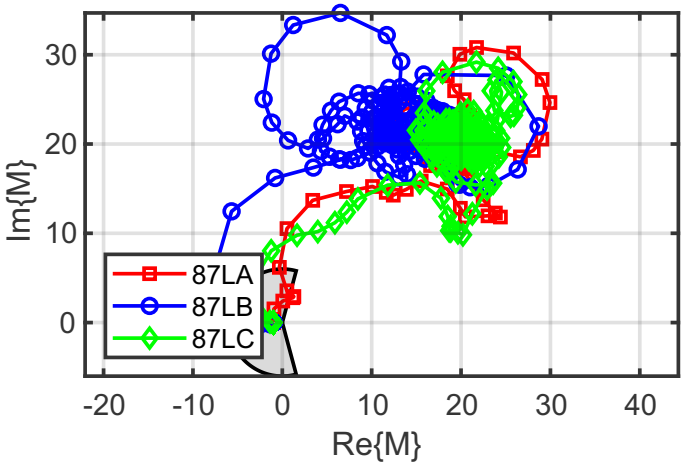

(a) Local terminal

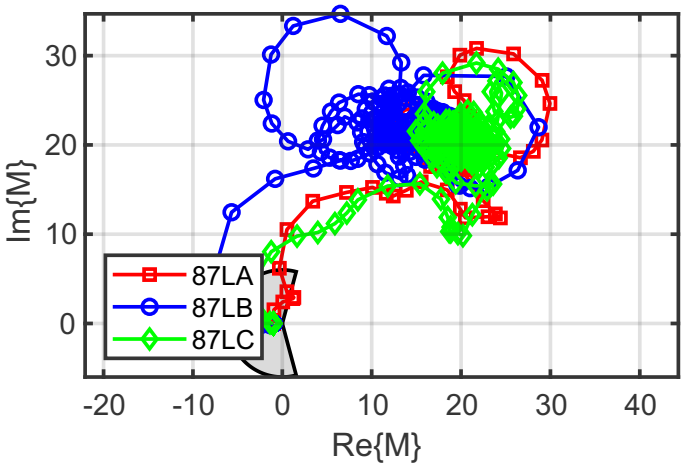

(b) Remote terminal

Figure 4.25. Case 5 - Alpha plane-based phase differential elements.

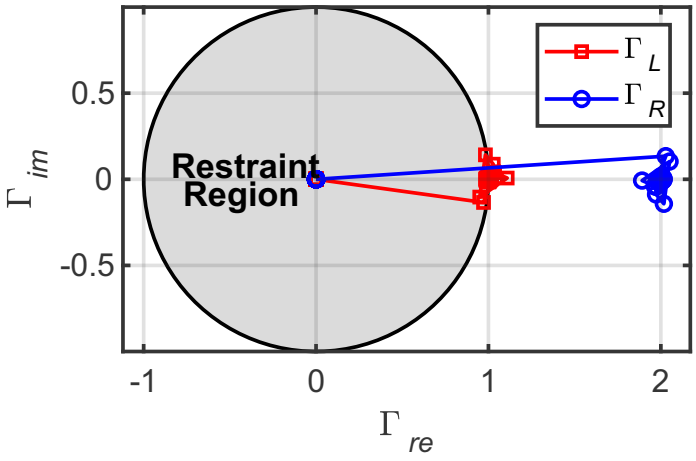

Figure 4.26. Case 5 - Proposed algorithm.

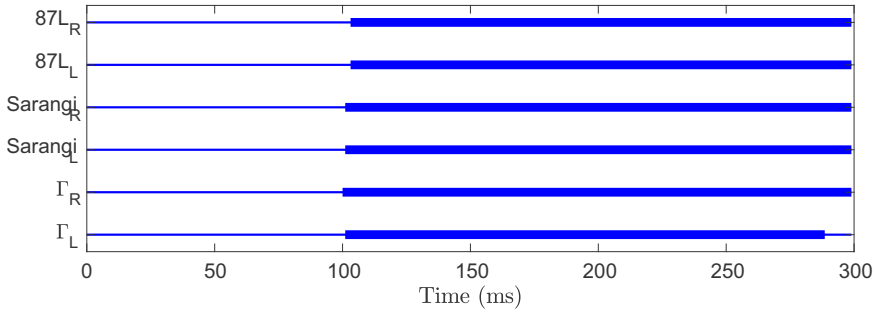

Figure 4.27. Case 5: Algorithms comparison.

4.1.5 Case 6 - Fault Transient Analysis - External Fault

In this case, aiming to verify the security of the evaluated algorithms, it was simulated an external 3P fault at the remote bus (i.e. Presidente Dutra station) with a fault resistance of 150 Ω. FigUures. 4.28 and 4.29 present the local and remote terminals currents and voltages during the external 3P fault at the remote bus.

In Figure 4.30, the behavior of local and remote phase units are observed. As one can see, the phase units correctly restrict the differential protection element. From Figure 4.31, it can be seen that the proposed algorithm operates correctly, forcing coefficients Γ_L and Γ_R to stay inside the restraint characteristic. Finally, from Figure 4.32, one can see that all the evaluated elements operates as expected, not issuing a trip command for the external fault.

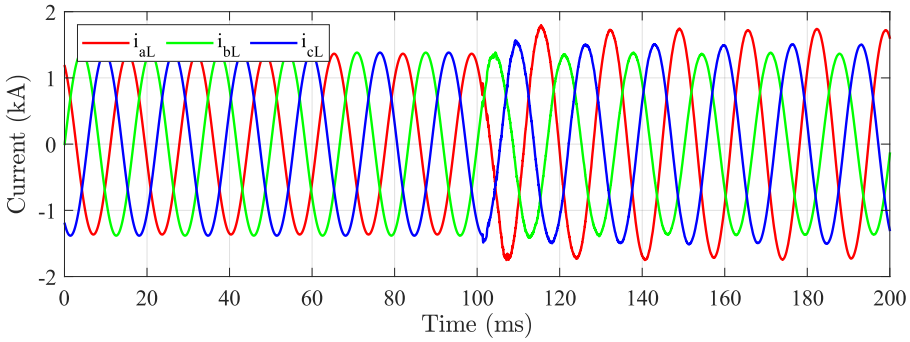

(a) Currents

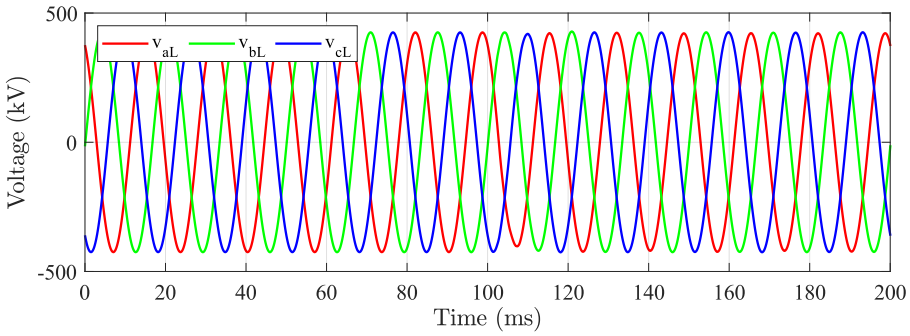

(b) Voltages

Figure 4.28. Case 6 - Local currents and voltages

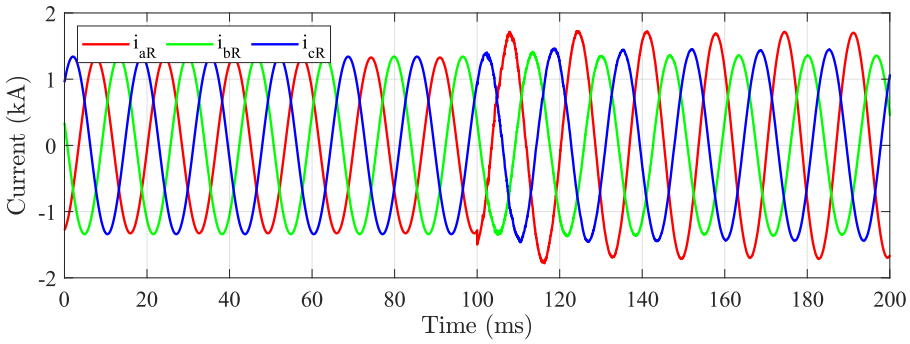

(a) Currents

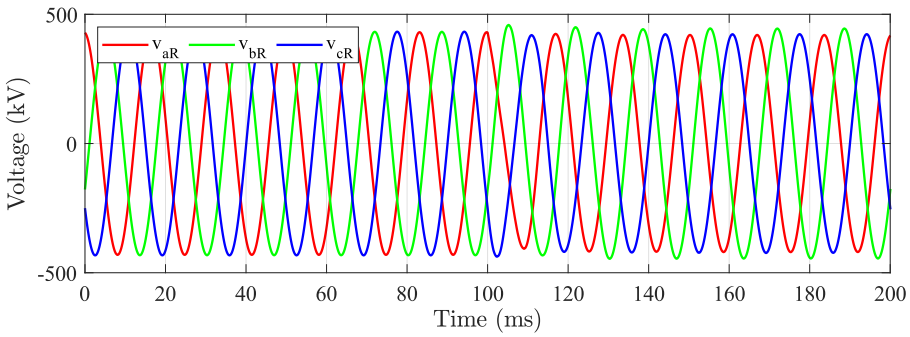

(b) Voltages

Figure 4.29. Case 6 - Remote currents and voltages

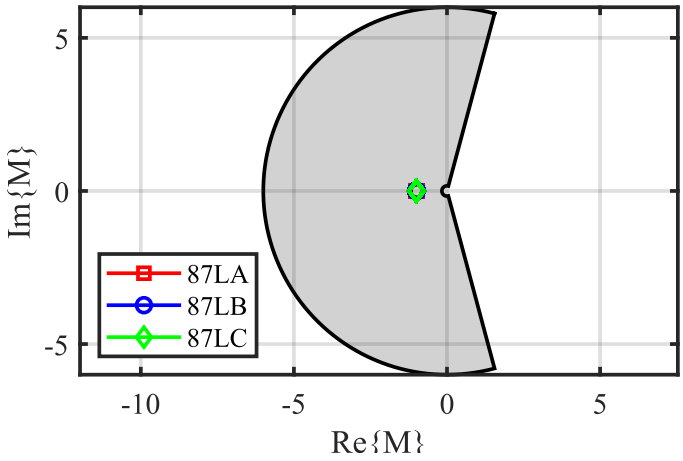

(a) Local terminal

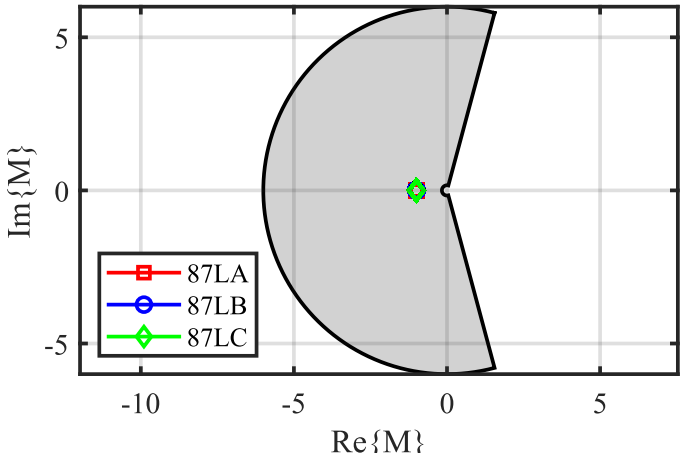

(b) Remote terminal

Figure 4.30. Case 6 - Alpha plane-based phase differential elements.

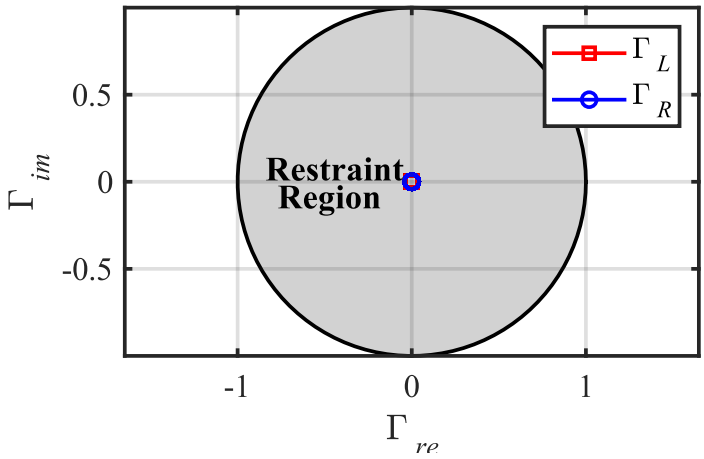

Figure 4.31. Case 6 - Proposed algorithm.

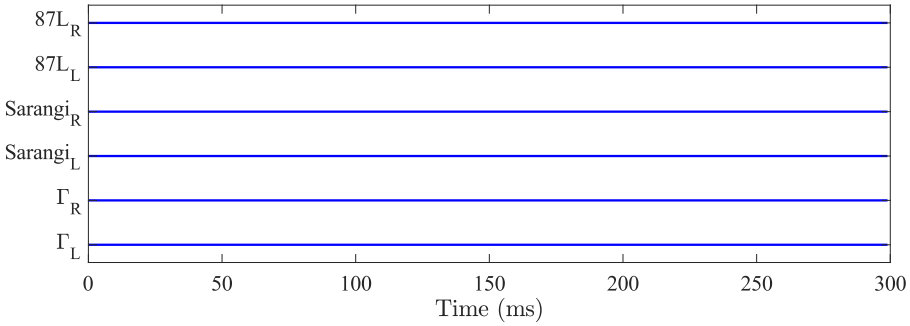

Figure 4.32. Case 6 - Algorithms comparison.

4.2 PARAMETRIC SENSITIVITY ANALYSIS

The following cases present the parametric sensitivity analyses (PSA). To thoroughly assess the performance of the algorithms, faults were simulated in a simplified system presented in Fig. 4.33. This system, also implemented in ATPDraw, consists in an homogeneous 500 kV system with a transmission line 400 km long, modeled as perfectly transposed with distributed and frequency-independent parameters. The CT and CCVT models reported in (IEEE POWER SYSTEM RELAYING COMMITTEE, 2004) and (PAJUELO et al., 2008), respectively, were also included in the simplified system.They are connected in series to the circuit breakers with the function of measuring the primary current that passes through the LT terminal and transforming it into secondary current values to be measured by the protection relays. The models of the capacitive potential transformers used are presented by (PAJUELO et al., 2008) with the function of measuring the primary voltage of the terminal and transforming it into secondary voltage values to be measured by the protection relays. It is worth noting that the subscripts 0 (zero) and 1 (one) correspond to the zero and positive sequence components, in that order.

At the line terminals, Thévenin equivalent circuits are represented, whose impedances are defined by means of the SIR (System-to-line Impedance Ratio), which is calculated as the ratio between the source and line impedances, from where the notation S_L for the local terminal and S_R for the remote terminal comes from.

A wide variety of faults were investigated, and the simulated short-circuit conditions considered the influence of some fault-related parameters, such as: fault type (three-phase, two-

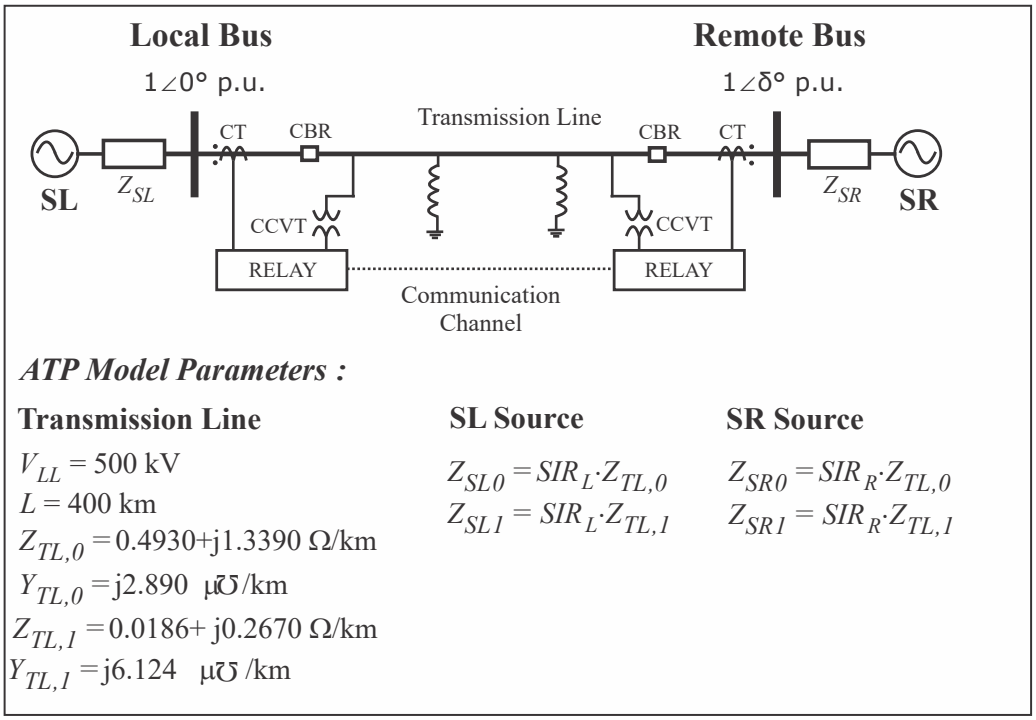

Figure 4.33. Simplified system

phase with or without ground, and single-phase), fault location (l), fault resistance (R_f), source strength (simulated by varying SIR_L and SIR_R) and system loading conditions (δ), which is determined assuming the local bus with voltage equal to $1\angle 0°$pu and the remote bus with $1\angle\delta$pu. It is noteworthy that the value assigned to δ corresponds to the angular phase shift between the bus voltages, and this adjustment is possible by controlling the voltages in the local and remote sources in steady state. Still on the short-circuits analyzed, it is worth mentioning that all phases were equally evaluated in all different types of fault.

To perform the PSAs, first, a one-line base case implemented in ATP and configured to provide the desired outputs in the COMTRADE format is defined. In the development of this case, the PARAMETER routine is used to parameterize variables such as angle, source strength, fault type, fault resistance, fault application location, among others. Using a spreadsheet created in the EXCEL software, the base case is replicated with changes in the variables of interest, generating a bank of ATP files for each case. These are simulated sequentially by means of a .bat routine that automates the simulation. Finally, the results are evaluated in the formulation proposed in this work.

An important aspect of PSAs is the possibility of identifying the influence of different parameters related to the short circuit or the influence of possible system operating configurations.

To obtain more comprehensive observations, only one parameter was varied at a time, while the others were kept constant.

The parameters evaluated in the PSA, as well as their values, are presented in Tab.4.1.

Table 4.1. Values assigned to Variables.

Simulation Variables	**Adopted Values**
Fault Resistance (R_f)	Phase-Phase:0,5,..,30 ,50,100,250. (Ω)
	Phase-Earth :0,5,...,45,100,250,300,400,500. (Ω)
Fault Location (l)	0,001;1;..,89,99. (% of the line)
System Loading (δ)	-90, -85,..,+85, +90. ($^\circ$)
Source Force (SIR)	0,1; 0,2;...;0,9 e 1; 2;...; 10

Regarding the values established for δ in Table 4.1, it is noteworthy that, although loading angles in the range $-90^\circ < \delta < 90^\circ$ were evaluated, in practice they are typically limited to $\pm 35^\circ$ (SAADAT, 2010). It is also worth mentioning that the source strength variation is performed separately for each of the sources, so that while the SIR of one of them is varied, that of the other remains unchanged. Furthermore, the source strength variation is always performed considering the same loading value. Thus, the equivalent impedances of the analyzed source are calculated depending on the value of SIR_L and also on the value of the loading to be evaluated and, based on these parameters, the voltages in the analyzed source are determined. The variation in system loading is determined by setting a voltage at the local bus equal to $1\angle 0^\circ$ p.u. and at the remote bus with $1\angle \delta^\circ$ p.u. The value assigned to δ corresponds to the angular phase shift between the bus voltages, a fact that is possible through the control of the voltage of local and remote sources in a steady state.

In this work, 5 cases are analyzed, which are described in Table 4.2. It is worth noting that the results of the proposed algorithm will be compared with the differential protection in the α-plane, since this is a unitary protection function like the one proposed in this work.

Table 4.2. Simulated Cases

Case	Type of fault	l	R_f	SIR_L	SIR_R	δ
PSA.1	BC	10 %	180,0	1,0	0,1	varies
PSA.2	AT	50 %	varies	0.1	0,1	$-15°$
PSA.3	ABC	varies	30,0	0,1	1,0	$-30°$
PSA.4	AT	varies	150,0	0,1	0,1	$-30°$
PSA.5	AT	50%	50,0	varies	1.0	$-15°$

4.2.1 PSA.1 - Load variation

This case presents the influence of loading in the correct performance of the proposed algorithm. Therefore, for this situation, the remote angle (δ) varies from $-90°$ to $90°$ with a step of $5°$. The local terminal source was considered with the $SIR_L = 1.0$ (weak source), and the remote source was considered with $SIR_R = 0.1$ (strong source). For this case, a BC fault in 10% of the line with fault resistance of 180 Ω was considered. The results are presented in Figures. 4.34, 4.35 and 4.36.

Based on the results presented in Figure 4.34, it is noted that the conventional alpha plane-based phase differential elements have correct performance for the healthy phases, as they remain at the stability point (0,0). However, for the faulted phases, the correct performance is limited to an interval of remote angle values, since the point lies inside the restraint characteristic.

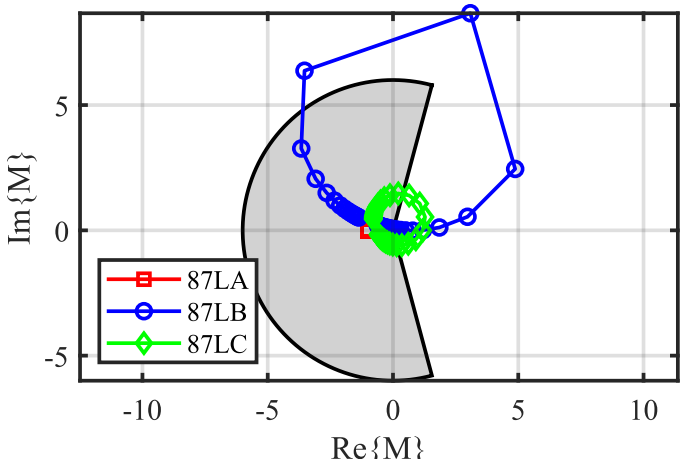

(a) Local terminal

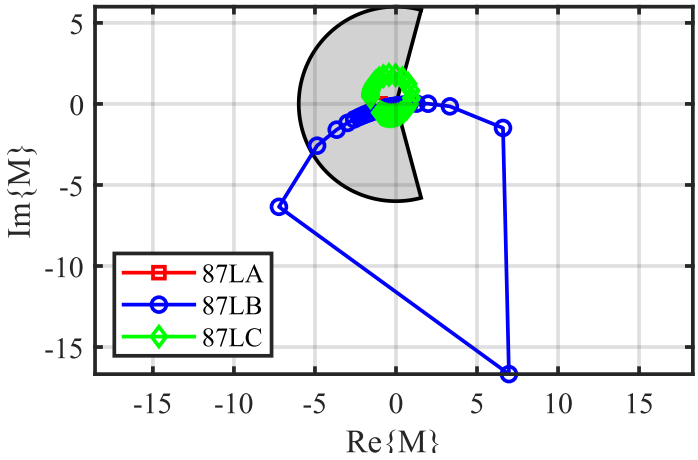

(b) Remote terminal

Figure 4.34. PSA.1 - Alpha plane-based phase differential elements.

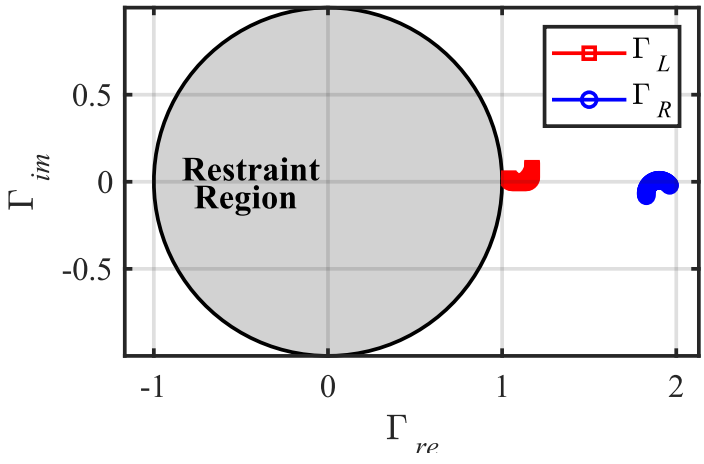

Figure 4.35. PSA.1- Proposed algorithm.

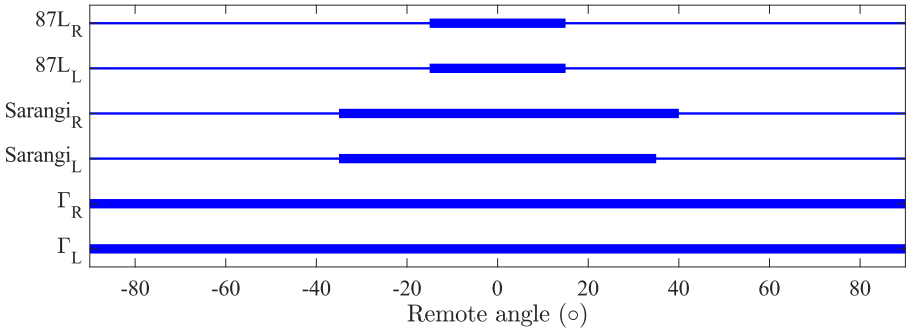

Figure 4.36. PSA.1 - Algorithms comparison.

From the analysis of Figure 4.35, which presents the behavior of the proposed algorithm, it can be seen that Γ_L and Γ_R operated for all simulated cases, since both coefficients lie outside of the restraint region. It is also noteworthy to point out that if one of the coefficients leaves the restraint area, the fault will then be detected, and a trip command is issued to the local circuit breakers (CBs) and to the remote ones through direct transfer trip (DTT).

In Figure 4.36, the proposed algorithm performance is compared with the conventional alpha plane-based phase differential elements and the alpha plane-based adaptive algorithm reported in (SARANGI; PRADHAN, 2017). It is observed that coefficients Γ_L and Γ_R operate correctly for δ varying from $-90°$ to $90°$. On the other hand, local and remote alpha plane-based phase differential elements only detected the fault for δ in between $-15°$ and $+15°$, whereas the algorithm reported in (SARANGI; PRADHAN, 2017) identified the fault in between $-35°$ and $+35°$, for the local terminal, and from $-35°$ and $+40°$ for the remote terminal. It occurs because the algorithm reported in (SARANGI; PRADHAN, 2017) is sensitive to source strength, and in Case 1 the strength of local and remote sources are different. Therefore, it can be seen that the proposed algorithm has a quite superior performance in comparison with the other evaluated algorithms regarding loading conditions.

4.2.2 PSA.2 - Fault Resistance Variation

This case aims to assess the influence of fault resistance on the evaluated algorithms. To do so, the fault resistance was varied from 0 to 500 Ω (with a step of 5Ω) for an AG fault in 50% of the line, with both sources set as strong (i.e., $SIR_L = 0.1$ and $SIR_R = 0.1$), and $\delta = -15°$ (i.e., light loading).

According to the results presented in Figures 4.37 and 4.38, the conventional alpha plane-based phase differential elements have correct performance for the healthy phases, as they remain at the stability point (0,0). However, for the faulted phase, it is observed that it loses sensitivity, because its trajectory moves towards inside the restraint characteristic from a certain fault resistance value, no more detecting the fault.

From analysis of Figure 4.38, which presents the performance of the proposed algorithm, it can be seen that the trajectories of Γ_L and Γ_R for fault resistance varying from 0 to 500 Ω lie outside of the restraint region for all fault resistance values. It is important to highlight that both Γ_L and Γ_R are fixed at 1.5, showing that the fault resistance parameter does not influence the algorithm performance, since H_L and H_R locate the defect correctly within 0.5 pu for a short circuit in 50% of the transmission line for the entire range of fault resistance variation.

In Figure 4.39, the proposed algorithm performance is compared with the conventional alpha plane-based phase differential element and the alpha plane-based adaptive algorithm reported in (SARANGI; PRADHAN, 2017). It is observed that, as aforementioned, coefficients Γ_L and Γ_R operated correctly for all fault resistances. Regarding conventional alpha plane-based phase differential elements and the algorithm reported in (SARANGI; PRADHAN, 2017), it is observed that both were capable of detecting faults with fault resistances ranging from 0 to 145 Ω. This same performance for both algorithms is because the fault takes place in the middle of the line and sources behind its terminals have the same strength (i.e., $SIR_L = 0.1$ and $SIR_R = 0.1$), so that pure fault currents coming from local and remote terminals are approximately equal. Based on these results, it can be seen that the proposed algorithm is more robust to fault resistance in comparison with the conventional alpha plane-based phase differential elements and the alpha plane-based adaptive algorithm reported in (SARANGI; PRADHAN, 2017).

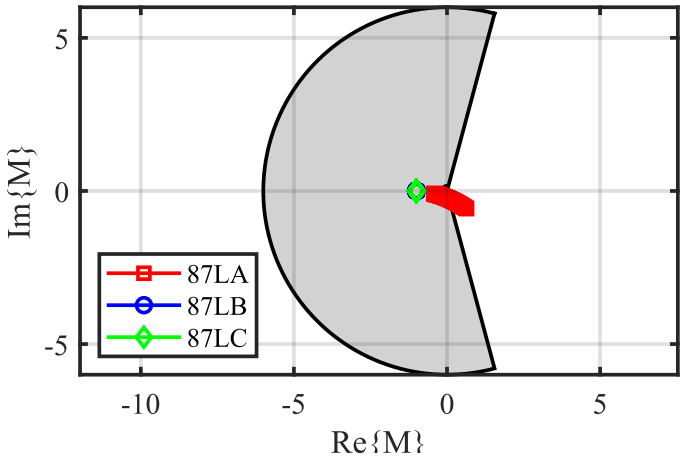

(a) Local terminal

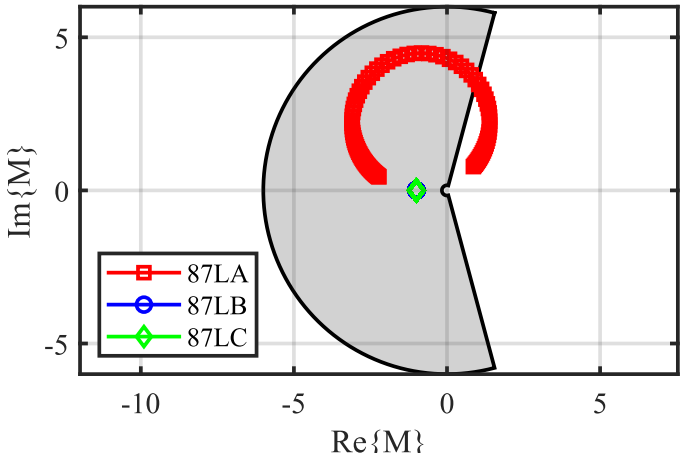

(b) Remote terminal

Figure 4.37. PSA.2 - Alpha plane-based phase differential elements.

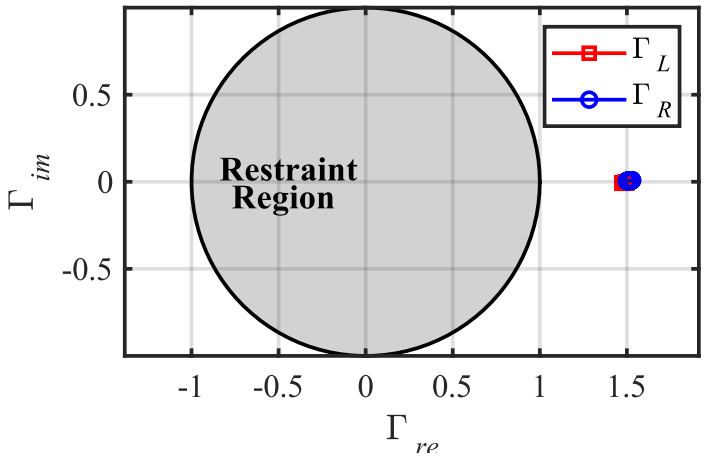

Figure 4.38. PSA.2- Proposed algorithm.

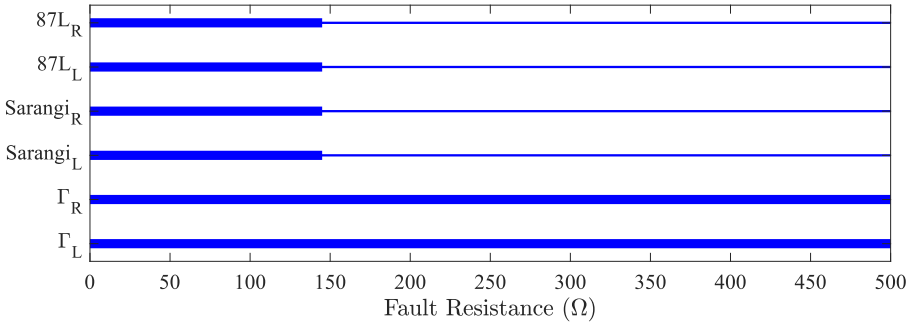

Figure 4.39. PSA.2 - Algorithms comparison.

4.2.3 PSA.3 e PSA.4 - Fault Location Variation

This case aims to evaluate fault location influence on the behavior of the proposed algorithm. Therefore, it was varied from 1 to 99% of the transmission line (with steps of 1%). Here, results from two fault types are presented: for an internal 3P fault, with fault resistance of 30 Ω and strong local source ($SIR_L = 0.1$) and weak remote source ($SIR_R = 1.0$); for an internal AG fault with fault resistance of 150 Ω and strong sources in both line terminals ($SIR_L = 0.1$ and $SIR_R = 0.1$). Results for the 3P fault are shown in Figures. 4.40, 4.41 and 4.42, whereas results for the AG fault are depicted in Figures. 4.43, 4.44 and 4.45.

It can be seen that for the 3P case shown in Figure. 4.40, the conventional alpha plane-based phase differential elements do not lose sensitivity to the variation of fault location. Conversely, in the case of the AG fault, it is observed from Figure 4.43 that the phase differential elements are influenced by the fault location, as they fail to detect faults for the entire line.

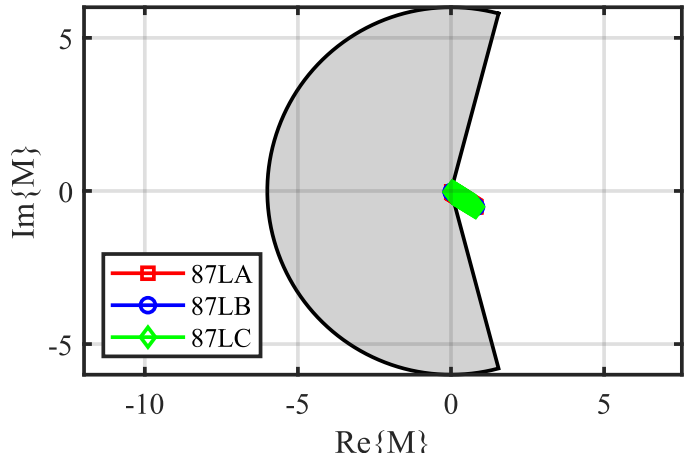

(a) Local terminal

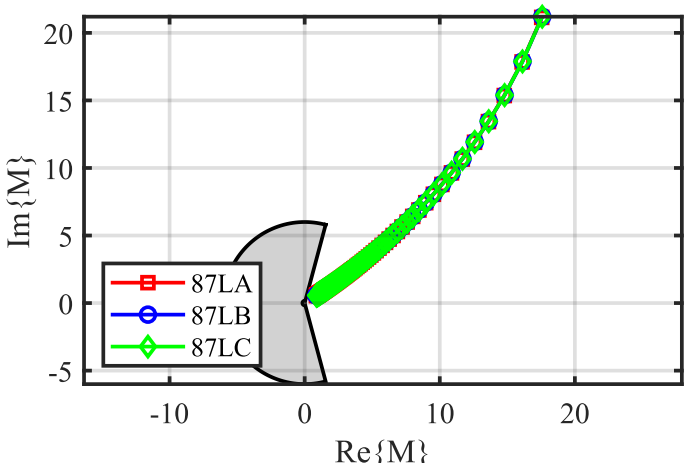

(b) Remote terminal

Figure 4.40. PSA.3 - 3P fault - alpha plane-base phase differential elements.

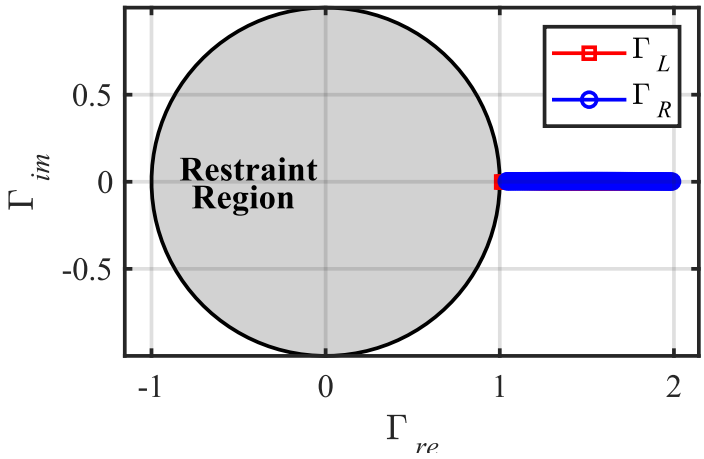

Figure 4.41. PSA.3 - 3P fault: proposed algorithm performance.

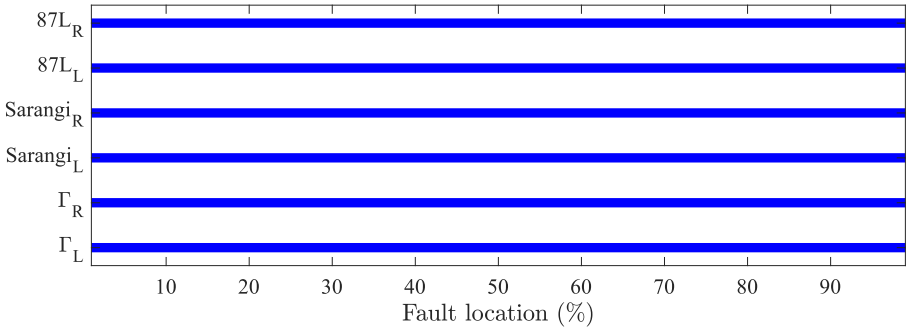

Figure 4.42. PSA.3- 3P fault - algorithms comparison.

Evaluating the proposed algorithm, in the case of 3P fault presented in Figure 4.41, it is observed that the coefficients Γ_L and Γ_R move outside the restraint region, showing the correct performance of the protection. For the AG fault case, the proposed algorithm also operates correctly for faults taking place on the entire line, as illustrated in Figure 4.44.

By the performance analysis of the algorithms in the case of the 3P fault depicted in Fig. 4.42, one can see that both conventional alpha plane-based phase differential elements and the algorithm reported in (SARANGI; PRADHAN, 2017) operated correctly for all faults, as well as the proposed algorithm. Nevertheless, by the analysis of the results for the AG fault, shown in Figure 4.45, it is observed that the conventional alpha plane-based phase differential elements lose their sensitivity for faults taking place in between 1% and 19% of the line. It is because these elements are sensitive to high fault resistances combined with high system loading and weak sources, which usually leads to outfeed condition during the fault, whereas the algorithm reported in (SARANGI; PRADHAN, 2017) was proposed to overcome this drawback. On the other hand, the proposed algorithm has provided quite robust performance regarding fault resistance for all evaluated cases, not only for those described in this paper.

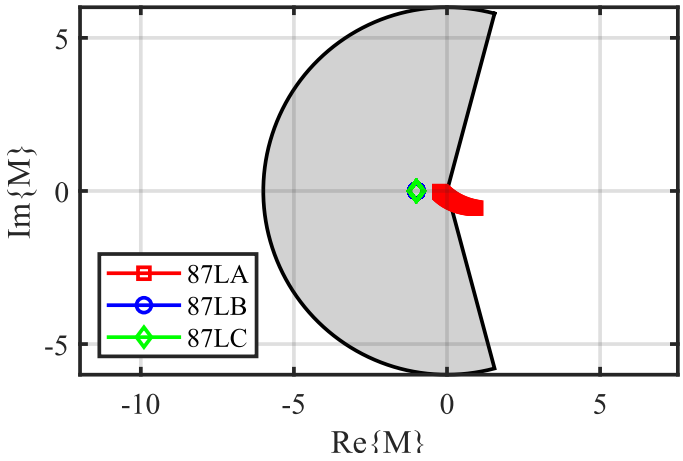

(a) Local terminal

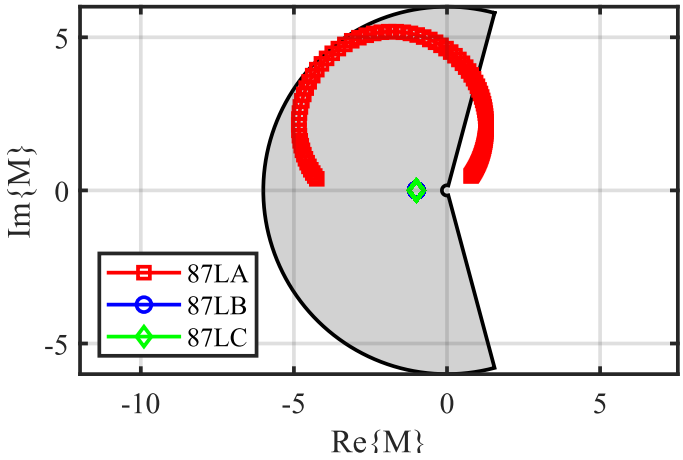

(b) Remote terminal

Figure 4.43. PSA.4 - AG fault - alpha plane-base phase differential elements.

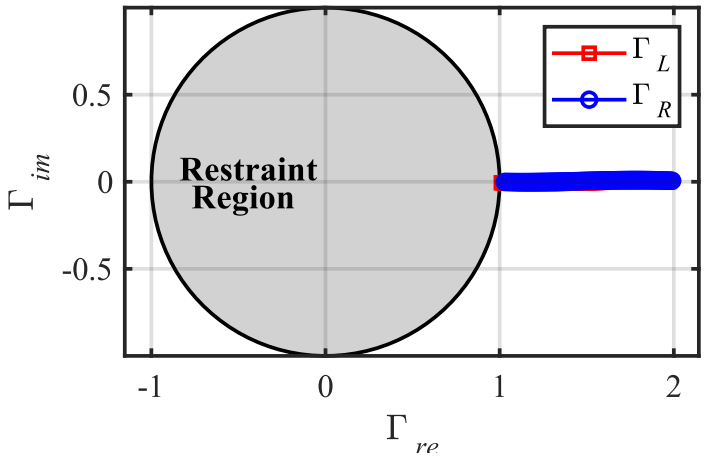

Figure 4.44. PSA.4 - AG fault: proposed algorithm performance.

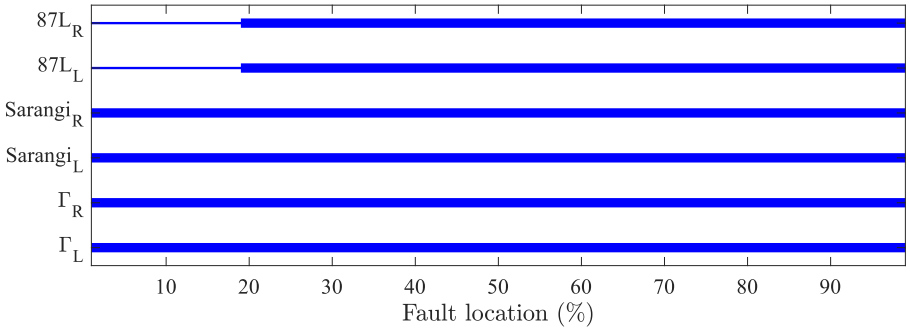

Figure 4.45. PSA.4 - AG fault: algorithms comparison.

4.2.4 PSA.5- Source Strength Variation

This case is simulated with the aim of evaluating the influence of the local terminal source strength on the algorithms. Thus, the parameter SIR_L was varied from 0.1 to 1.0 in steps of 0.1, and from 1.0 to 10.0 in steps of 1.0, keeping the remote source strong ($SIR_R = 0.1$). An internal AG fault at 50 % of the line with fault resistance of 50 Ω and remote angle $\delta = -15°$ were considered. It should be noted that the fault was simulated halfway across the line precisely, so that there is no influence of fault location on this analysis.

In Figure 4.46, it can be seen that the conventional alpha plane-based phase differential elements for the healthy remain stable into the restraint characteristic. However, the trajectory for the faulted phase reveals this element fails to detect the fault from a certain value of SIR_R, since the point moves toward inside the restraint characteristic. Conversely, one can see that coefficients Γ_L and Γ_R of the proposed algorithm operated correctly for all values of SIR_R, as shown in Fig. 4.47.

From Figure 4.48, it is observed that coefficients Γ_L and Γ_R operated correctly for all range of SIR_R, as aforementioned. On the other hand, the conventional alpha plane-based phase differential elements and the remote element of the algorithm reported in (SARANGI; PRADHAN, 2017) fail to detect faults for $SIR_R > 5.0$.

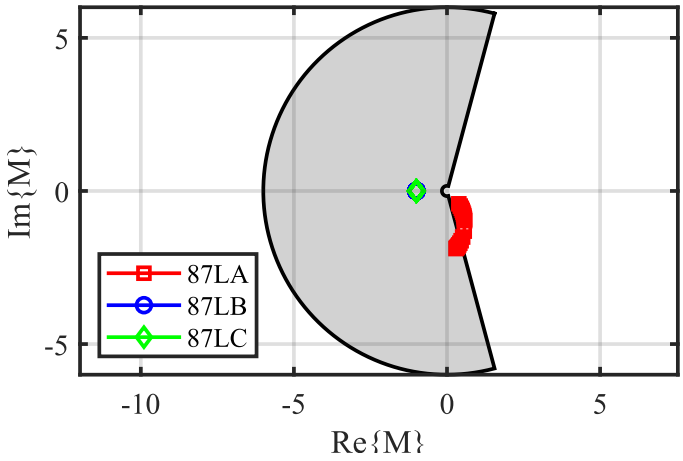

(a) Local terminal

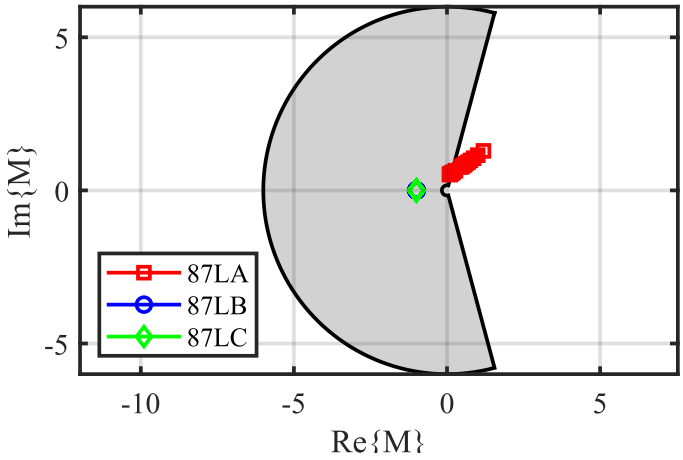

(b) Remote terminal

Figure 4.46. PSA.5- alpha plane-based phase differential elements.

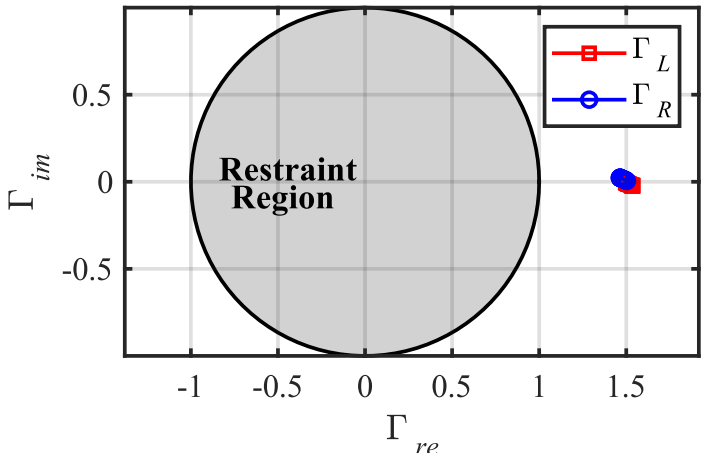

Figure 4.47. PSA.5 - Proposed algorithm.

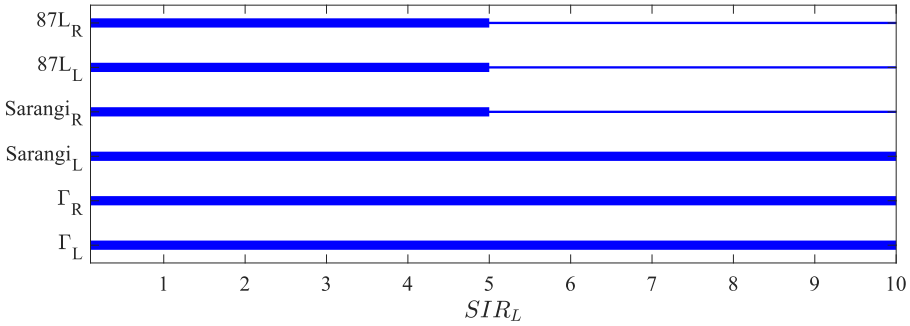

Figure 4.48. PSA.5- algorithms comparison.

CHAPTER 5

CONCLUSION AND FUTURE INVESTIGATIONS

This thesis presented a new unit protection algorithm for transmission lines, which combines characteristics of both distance and differential protection, but in an innovative way. The algorithm calculates coefficients Γ_L and Γ_R, and a fault is detected whenever one of these coefficients moves towards outside the proposed restraint characteristic. It also uses a faulted phase selection combined with an external fault detection logic and a novel harmonic restraint strategy, providing dependability for internal faults and security to avoid misoperating for external faults with CT saturation.

The proposed algorithm was evaluated by means of faults simulated in the ATPDraw software. The transient performance of the proposed algorithm was assessed considering a realistic model of the Brazilian power grid, specially the 500 kV double-circuit series compensated line between Imperatriz and Presidente Dutra stations and power equipment in its vicinity.The performance of the proposed algorithm was further evaluated by considering parametric sensitivity analyzes in a simplified power system. Results reveals the proposed algorithm is quite robust to fault resistance, fault location, loading conditions and source strength, providing a much better performance in comparison with the conventional alpha plane-based phase differential elements and the alpha plane-based adaptive algorithm reported in (SARANGI; PRADHAN, 2017).

It is noteworthy that some vendors use on their relay alpha plane-based algorithms which provide quite similar performance of the conventional alpha plane-based phase differential elements evaluated here for internal faults in two-terminals lines. Therefore, the proposed algorithm seems to be quite promising to be used in real world transmission lines unit protection applications.

As a continuation of the studies carried out in this thesis, the following proposals are suggested of future work:

- Conduct tests to verify the possibility of integrating the algorithm into existing commercially available devices and evaluate its behavior using real oscillographic recordings.
- Evaluate the performance of the algorithm with another fault location strategy.
- Evaluate the performance of the proposed algorithm in multiple circuit systems and investigate possible adjustments necessary for its correct operation.
- Assess the impact of weak sources, such as renewable sources connected to the grid by inverters. In a scenario where solar and wind sources show a tendency for a significant increase in participation in the global energy matrix in the coming decades.

REFERENCES

ABDELSALAM, H.; ABDIN, A.; BADR, M. *A Fault Resistance Compensation Algorithm Based on a Digital Distance Relaying Scheme*. 2018. 415-421 p. Cited 2 times in pages 6 and 9.

ALMEIDA, M.; SILVA, K. Transmission lines differential protection based on an alternative incremental complex power alpha plane. *IET Generation, Transmission Distribution*, v. 11, n. 1, p. 10–17, 2017. Cited 2 times in pages 11 and 13.

ALTUVE, H.; BENMOUYAL, G.; ROBERTS, J.; TZIOUVARAS, D. A. Transmission line differential protection with an enhanced characteristic. v. 2, p. 414–419 Vol.2, April 2004. Cited 2 times in pages 8 and 13.

ALTUVE, H. J.; SCHWEITZER, E. O. *Modern Solutions for Protection, Control and Monitoring of Electric Power Systems*. Pullman, USA: Schweitzer Engineering Laboratories, Inc., 2010. No citation in text.

ANDERSON, P. M. *Power System Protection*. Piscataway, New Jersey, EUA: John Wiley & Sons Inc., 1999. Cited in page 2.

BAINY, R.; SILVA, K. Enhanced generalized alpha plane for numerical differential protection application. *IEEE Transactions on Power Delivery*, p. 1–1, 2020. Cited 2 times in pages 12 and 13.

BENMOUYAL, G. *The Trajectories of Line Current Differential Faults in the Alpha Plane*. Schweitzer Engineering Laboratories Inc., Pullman, WA, 2005. Cited 2 times in pages 8 and 13.

DANTAS, D.; PELLINI, E.; MANASSERO, G. Time-domain differential protection method applied to transmission lines. *IEEE Transactions on Power Delivery*, v. 33, n. 6, p. 2634–2642, 2018. Cited 2 times in pages 11 and 13.

EISSA, M. *Ground distance relay Compensation baseada no cálculo de resistência de falha*. 2006. 1830-1835 p. Cited 2 times in pages 4 and 9.

FILOMENA, A.; SALIM, R.; RESENER, M.; BRETAS, A. *Ground Distance Relaying with Fault-Resistance Compensation for Unbalanced Systems*. 2008. 1319-1326 p. Cited 2 times in pages 4 and 9.

GUPTA, R.; ALI, S.; KAPOOR, G. A novel current differential relaying scheme for transmission line protection. p. 1–6, 2020. Cited 2 times in pages 12 and 13.

ABB POWER T&D COMPANY INC. David G. Hart, Damir Novosel & Robert A. Smith. *Modified Cosine Filters*. 2000. US00615487A, apr. 15, 1998, Nov. 28, 2000. No citation in text.

HOSSAIN, M.; LEEVONGWAT, I.; RASTGOUFARD, P. Revisions on alpha plane for enhanced sensitivity of line differential protection. *IEEE Transactions on Power Deliver*, v. 33, n. 6, p. 3260–3262, 2018. Cited 2 times in pages 11 and 13.

IDRIS, M.; AHMAD, M.; ABDULLAH, A.; HARDI, S. *Adaptive Mho type distance relaying scheme with fault failurepensions*. 2013. 213-217 p. Cited 2 times in pages 5 and 9.

IEEE POWER SYSTEM RELAYING COMMITTEE. *EMTP Reference Models for Transmission Line Relay Testing*. [S.l.], 2004. Cited in page 35.

LIANG, Y.; LI, W.; LU, G. X. Z.; WANG, C. A new distance protection scheme based on improved virtual measured voltage. *IEEE Transactions on Power Delivery*, v. 35, n. 2, p. 774–786, April 2019. Cited 2 times in pages 7 and 9.

LIANG, Y.; LU, Z.; LI, W.; ZHA, W.; HUO, Y. *A Novel Fault Impedance Calculation Method for Distance Protection Against Fault Resistance*. 2020. 396-407 p. Cited 2 times in pages 7 and 9.

LIU, Q.; HUANG, S.; LIU, H.; LIU, W. *Adaptive Impedance Relay With Composite Polarizing Voltage Against Fault Resistance*. 2008. 586-592 p. Cited 2 times in pages 10 and 13.

MA, J.; MA, W.; QIU, Y.; THORP, J. *An Adaptive Distance Protection Scheme Based on the Voltage Drop Equation*. 2015. 1931-1940 p. Cited 2 times in pages 5 and 9.

MA, J.; XIANG, X.; LI, P.; DENG, Z.; THORP, J. *Adaptive distance protection scheme with quadrilateral characteristic for extremely high-voltage/ultra-high-voltage transmission line*. 2017. 1624-1633 p. Cited 2 times in pages 6 and 9.

MA, J.; YAN, X.; FAN, B.; LIU, C.; THORP, J. *A Novel Line Protection Scheme for a Single Phase-to-Ground Fault Based on Voltage Phase Comparison*. 2016. 2018-2027 p. Cited 2 times in pages 6 and 9.

MAKWANA, V. H.; BHALJA, B. R. *A New Digital Distance Relaying Scheme for Compensation of High-Resistance Faults on Transmission Linea*. 2012. 2133-2140 p. Cited 2 times in pages 5 and 9.

MILLER, H.; BURGER, J.; FISCHER, N.; KASZTENNY, B. Modern line current differential protection solutions. In: TEXAS A&M CONFERENCE FOR PROTECTIVE RELAY ENGINEERS. Texas, USA, 2010. Cited 3 times in pages 10, 13, and 31.

MOLAS, E. C.; MORAIS, L. P.; SILVA, K. M. Análise das trajetórias no plano alfa referentes operação da proteção diferencial de linhas de transmissão. In: SEMINÁRIO NACIONAL DE PRODUÇÃO E TRANSMISSÃO DE ENERGIA ELÉTRICA (XXII SNPTEE). Brasília, DF, 2013. Cited 2 times in pages 10 and 13.

NAIDU, O. D.; GEORGE, N.; ZUBIC, S.; KRAKOWSKI, M. Time-domain-based distance protection for transmission networks: Secure and reliable solution for complex networks. *IEEE Access*, v. 11, p. 104656–104675, 2023. Cited 2 times in pages 8 and 9.

PAINTHANKAR, Y. G.; BHIDE, S. R. *Fundamentals of Power System Protection*. New Delhi, India: Prentice-Hall, 2007. Cited in page 1.

PAJUELO, E.; RAMAKRISHNA, G.; SACHDEV, M. S. Phasor estimation technique to reduce the impact of coupling capacitor voltage transformer transients. *IET Generation, Transmission & Distribution*, v. 2, 2008. Cited in page 35.

ROBERTS, J.; GUZMAN, A.; SCHWEITZER, E. O. Z=v/i does not make a distance relay. In: 20TH ANNUAL WESTERN PROTECTIVE RELAY CONFERENCEE. Spokane, Washington, 1993. No citation in text.

SAADAT, H. *Power System Analysis*. 3. ed. Minnesota, USA: PSA Publishing, 2010. No citation in text.

SARANGI, S.; PRADHAN, A. K. Adaptive -plane line differential protection. *IET Generation, Transmission & Distribution*, v. 11, n. 10, p. 2468–2477, 2017. Cited 11 times in pages 11, 13, 35, 36, 42, 45, 59, 60, 64, 66, and 69.

SILVA, K.; BAINY, R. Generalized alpha plane for numerical differential protection applications. *IEEE Transactions on Power Delivery*, v. 31, n. 6, p. 2565–2566, 2016. Cited 2 times in pages 10 and 13.

SILVA, K.; BAINYA, R. Generalized alpha plane for numerical differential protection applications. *IEEE Transactions on Power Delivery*, v. 31, n. 6, p. 2565–2566, 2016. Cited in page 12.

SONG, G.; CHU, X.; GAO, S.; KANG, Z. J. X.; SUONAN, J. *Novel Distance Protection Based on Distributed Parameter Model for Long-Distance Transmission Lines*. 2013. 2116-2123 p. Cited 2 times in pages 5 and 9.

TIFERES, R. R.; MANASSERO, G. Time-domain differential protection of transmission lines based on bayesian inference. *IEEE Transactions on Power Delivery*, v. 37, n. 3, p. 1569–1577, 2022. Cited 2 times in pages 12 and 13.

TZIOUVARAS, D. A.; ALTUVE, H.; BENMOUYAL, G.; ROBERTS, J. *Line Differential Protection with an Enhanced Characteristic*. Schweitzer Engineering Laboratories Inc., Pullman, WA, 2003. Cited 2 times in pages 8 and 13.

VASQUEZ, F. A. M.; SILVA, K. M. Instantaneous-power-based busbar numerical differential protection. *IEEE Transactions on Power Delivery*, v. 34, n. 2, p. 616–626, 2019. No citation in text.

WARRINGTON, A. R. C. *Protective Relays: Their Theory and Practice, Volume 1*. 1. ed. London: Chapman & Hall, 1962. No citation in text.

XU, Z.; XU, G.; RAN, L.; YU, S.; YANG, Q. *A New Fault-Impedance Algorithm for Distance Relaying on a Transmission Line*. 2010. 1384-1392 p. Cited 2 times in pages 4 and 9.

XU, Z. Y.; DU, Z. Q.; RAN, L.; WU, Y. K.; YANG, Q. X.; HE, J. L. A current differential relay for a 1000-kv uhv transmission line. *IEEE Transactions on Power Delivery*, v. 22, n. 3, p. 1392–1399, Jul 2007. Cited 2 times in pages 9 and 13.

XUE, Y.; KASZTENNY, B.; TAYLOR, D.; XIA, Y. *Series Compensation, Power Swings, and Inverter-Based Sources and Their Impact on Line Current Differential Protection*. Pullman, WA, 2013. Cited 2 times in pages 10 and 13.

ZHENG, Y.; WU, T.; HONG, F.; YAO, G.; CHAI, J.; WEI, Z. Transmission line distance protection under current transformer saturation. *Journal of Modern Power Systems and Clean Energy*, p. 68–76, 2021. Cited 2 times in pages 7 and 9.

ZIEGLER, G. *Numerical Distance Protection: Principles and Applications*. Germany: Siemens, 2006. Cited in page 2.

ZIEGLER, G. *Numerical Differential Protection: Principles and Applications*. 2nd. ed. Berlin, Germany: Siemens, 2012. Cited in page 2.